Mathematical models for the study of synchronization phenomena in neuronal networks

Roberta Sirovich

Mathematical models for the study of synchronization phenomena in neuronal networks

Modèles mathématiques
pour l' étude des phénomènes de synchronisation
dans les réseaux neuronaux

Thèse de doctorat

présentée à
l' Università degli Studi di Torino et l' Université Grenoble I Joseph Fourier
par

Roberta Sirovich

Jury
Prof. Ferdinando Arzarello, Président
Prof. Petr Lánský, Rapporteur
Prof. Jean-Pierre Rospars, Rapporteur
Prof. Laura Sacerdote, Codirecteur de thèse
Prof. Alessandro E. P. Villa, Codirecteur de thèse
Dr. Patricia Duchamp-Viret, Expert

Torino et Grenoble 2005–2006

Mathematical models for the study of synchronization phenomena in neuronal networks

Roberta Sirovich

Dipartimento di Matematica, Università degli Studi di Torino
Laboratoire de Neurosciences Précliniques – INSERM U318, Université Grenoble 1

The spike train, i.e. the sequence of the action potential timings of a single unit (i.e. a single neuron in most cases), is the usual data that is analyzed in electrophysiological recordings for the description of the firing pattern which is supposed to characterize a certain type of cell. The statistical distribution of the interspike intervals (ISI) is a first order statistics that is often provided in experimental studies. However, its interpretation is far from being trivial and could reveal interesting phenomena associated to the underlying network activity. We present the results obtained describing the firing activity of a small network of neurons with a mathematical jump diffusion model. That is the membrane potential as a function of time is given by the sum of a stochastic diffusion process and two counting processes that provoke jumps of constant sizes at discrete random times. Different distributions are considered for such processes: jump processes with inter-events Exponentially and Inverse Gaussian distributed, Wiener and Ornstein Uhlenbeck diffusion processes. Moreover we consider two configuration of the small network: open circuit and close circuit. Two main results emerge. The first one is that interspike intervals (ISI) histograms show more than one peak (multimodality) and exhibit a resonant like behavior. This fact suggests that in correspondence of each mode (i.e. the lag of the maxima) the cell has a higher probability of firing such that the the lags become *characteristic times* of the cell which could be modulated under physiological conditions. The second main result concerns the role of inhibition in neuronal coding. Indeed we show that the inhibitory inputs may facilitate the transmission of the spikes generated by the excitatory unit. This fact suggests that inhibitory cells are not only involved in keeping balanced the excitability of the cell but that they may also play a key role in the information process.

The simulation of such kind of models requires to evaluate the first passage time through a threshold of a stochastic process. In this framework arises the necessity to improve classical algorithms with the evaluation of bridge process crossing probabilities. So that the second

part of this manuscript is dedicated to a purely theoretical study on multidimensional bridge processes associated to a regular diffusion process. The SDE fulfilled by the conditioned process is written, starting from the SDE giving the process on which the bridge is built. Two methods to have a version of the solution of the SDE giving the bridge are explored, i.e. the space time transformations and the conditioning of the solution of a suitable second order SDE with Dirichlet boundary conditions.

Modèles mathématiques pour l' étude des phénomènes de synchronisation dans les réseaux neuronaux

Roberta Sirovich

Dipartimento di Matematica, Università degli Studi di Torino
Laboratoire de Neurosciences Précliniques – INSERM U318, Université Grenoble 1

Les enregistrements électrophysiologiques extracellulaires permettent d'obtenir le soi-disant "train de spikes", c'est à dire la série temporelle des potentiels d'action d'un neurone, qui est supposée être l'une des caractéristiques fonctionnelles de l'activité neuronale. La distribution des intervalles entre deux décharges neuronales successives (ISI) est une statistique du premier ordre couramment utilisée dans les études expérimentales électrophysiologiques. Cependant, son interprétation est loin d'être banale et pourrait indiquer des phénomènes intéressants associés à l'activité fondamentale du réseau. Afin de mieux comprendre cette statistique, ce travail présente les résultats obtenus par l'étude de l'activité d'un micro réseau neuronal décrit par des équations mathématiques du type "saut-diffusion". La variation du potentiel membranaire du neurone en fonction du temps est donné par la somme d'un processus stochastique de diffusion et de deux processus de point, qui provoquent des sauts d'amplitude constante à des temps aléatoires discrets. Différentes distributions sont considérées pour ces processus: processus de saut avec inter-événements distribués exponentiellement ou par une fonction gaussienne inverse, processus de diffusion de Wiener ou d'Ornstein Uhlenbeck. Nous considérons aussi deux configurations de micro réseau: réseau ouvert ou réseau fermé, c'est à dire avec rétroaction du processus résultant sur les processus générateurs.

Ce travail fait ressortir deux résultats principaux. Le premier est que les histogrammes des ISI montrent plusieurs maxima et un comportement de type résonnant. En correspondance de chaque maximum la cellule a une probabilité plus élevée de se décharger, de manière que les latences des pics d'histogrammes représentent des temps caractéristiques de la cellule pouvant être modulés par diverses conditions physiologiques. Le deuxième résultat principal concerne le rôle de l'inhibition dans le codage neuronal. Nous avons démontré que, sous certaines conditions, les afférences inhibitrices peuvent faciliter la transmission des potentiels d'action propagés par les connexions excitatrices. De ce fait l'on déduit que les cellules inhibitrices ne doivent pas seulement être considérées pour leur rôle équilibreur vis-à-vis de l'excitabilité

générale des neurones mais également pour le rôle qu'elles peuvent jouer dans le traitement et le codage de l'information neuronale.

La simulation de ce type de modèles exige l'évaluation du temps de premier passage par le seuil d'un processus stochastique. Dans ce cadre surgit la nécessité d'améliorer les algorithmes classiques avec l'évaluation des probabilités de croisement du seuil par un processus "bridge", correspondant au processus de diffusion simulé. La deuxième partie de ce manuscrit est dédiée à une étude purement théorique sur les processus bridge multidimensionnels associés à un processus de diffusion régulier. Nous écrivons l'équation stochastique différentielle satisfaite par le processus bridge et proposons deux méthodes alternatives pour trouver une version de la solution dans le cas bidimensionnel. Toutes les méthodes présentées sont illustrées avec l'exemple du processus du mouvement brownien intégré.

Publications

[1] M. T. Giraudo, L. Sacerdote and R. Sirovich *Effects of random jumps on a very simple neuronal diffusion model.* BioSystems, **67** (2002), pp. 74-83.

[2] L. Sacerdote and R. Sirovich *A Wiener process with Inverse Gaussian time distributed jumps as a model for neuronal activity.* Proceedings of the 5th ESMTB Conference 2002, V.Capasso Editor.

[3] L. Sacerdote and R. Sirovich *Multimodality of the Interspike Interval Distribution in a simple jump-diffusion model.* Scientiae Mathematicae Japonicae, **8** (2003), pp. 359-374.

[4] R. Sirovich and L. Sacerdote *Noise induced phenomena in jump diffusion models for single neuron spike activity.* IJCNN2004 CD-ROM Conference Proceedings, IEEE Catalog Number 04CH37541C, ISBN: 0-7803-8360-5.

[5] R. Sirovich, L. Sacerdote and A.E.P. Villa *Multimodal inter-spike interval distribution in a jump-diffusion neuronal model.* Submitted for publication.

[6] R. Sirovich and C. Zucca *Multidimensional Bridges with application to the Integrated Brownian Motion.* Preprint.

Adresses

Président
Prof. **Ferdinando Arzarello**
Dipartimento di Matematica, Università degli studi di Torino
Via Carlo Alberto 10
10128 Torino, Italia.

Rapporteur
Prof. **Petr Lánský**
Institute of Physiology, Academy of Sciences of the Czech Republic
Videnska 1083
142 20 Prague 4, Czech Republic.

Rapporteur
Prof. **Jean-Pierre Rospars**
INRA - Unitè de Phytopharmacie et Médiateurs Chimiques
Route de St-Cyr
F-78026 Versailles cedex, France.

Codirecteur de Thèse
Prof. ssa **Laura Sacerdote**
Dipartimento di Matematica, Università degli studi di Torino
Via Carlo Alberto 10
10128 Torino, Italia.

Codirecteur de Thèse
Prof. **Alessandro E. P. Villa**
Inserm U318, Laboratoire de Neurosciences Précliniques
Universitè Joseph Fourier

CHU Grenoble Pavillon B
BP 217 38043 Grenoble cedex 9, France.

Expert

Dr. ssa **Patricia Duchamp-Viret**
Laboratoire de Neurosciences et Systémes Sensoriels
Universitè Claude Bernard
50, avenue Tony Garnier
F-69366 Lyon cedex 07.

RÉSUMÉ

Comprendre le fonctionnement du cerveau est l'un des défis scientifiques les plus importants. Jusqu'à la fin du XIXème siècle, et au début du XXème, les scientifiques n'étaient pas encore persuadés que le tissu cérébral était composés par des cellules. C'est le scientifique espagnol Santiago Ramón y Cajal, avec son remarquable travail histologique, qui convainquit la communauté scientifique que le cerveau était constitué par des cellules, les neurones, qui sont de véritables éléments unitaires et qui agissent l'un sur l'autre par des contacts spécialisés appelés synapses. Aujourd'hui nous savons que le tissu du cerveau se compose de deux types principaux de cellules, les cellules nerveuses, appelées neurones, et les cellules neurogliales, appelées généralement glie. La glie joue un rôle important, pas encore complètement compris, mais qui ne fait pas l'objet de cette étude. L'unité qui nous intéresse et qui traite principalement la transmission du signal, est le neurone. Mais qu'est-ce que c'est un *signal*?

Dynamique de la membrane neuronale

Dans le système nerveux humain il est possible de trouver près de 10^{12} neurones caractérisés par une diversité morphologique et fonctionnelle extraordinaire. Cependant, comme point de départ, nous allons décrire une cellule neuronale typique, et simplifiée, (cf. Figure 0.1), avec trois éléments fondamentaux: le corps de la cellule, appelé *soma*, qui est la partie de la cellule où se trouve le noyau; les *dendrites*, qui sont des appendices ramifiées donnant lieu à l'arbre *dendritique*, et où se produisent les contacts avec les autres cellules aux emplacements spécialisés appelés *synapses*; l'*axone* qui est une appendice particulière et unique, avec des branchements terminaux, par laquelle se propage le potentiel d'*action*. Il y a une différence de potentiel entre l'intérieur et l'extérieur de la cellule neuronale, mais ce qui caractérise un neurone est son excitabilité. Le courant électrique est porté par des ions, principalement le

sodium (Na), le potassium (K), le calcium (Ca) et le chlorure (Cl), qui traversent la membrane cellulaire dans certaines conditions. Même si les lois de la physique qui règlent les mouvements ioniques sont simples, les propriétés électrophysiologiques caractéristiques d'une cellule neuronale sont très complexes. La description analytique de la décharge d'une cel-

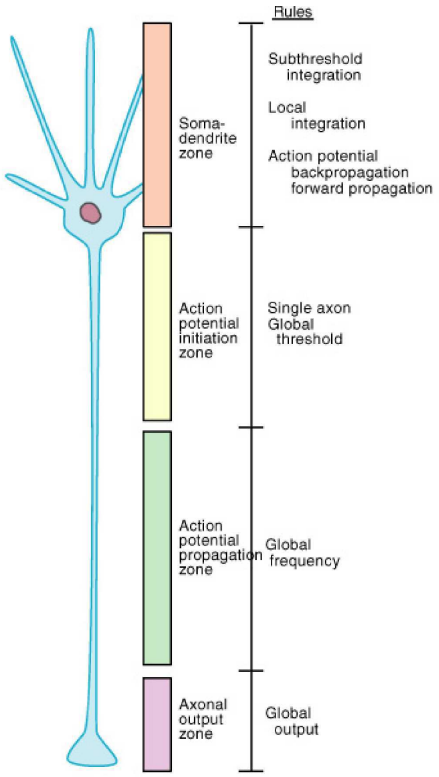

FIGURE 0.1. Représentation schématique d'une cellule neuronale typique.

lule neuronale porta A. L. Hodgkin et A. F. Huxley [**24**] à formuler les premières équations en fonction de la concentration différentielle des conductances ioniques et des concentrations des ions. La membrane du neurone peut être vue comme une série de capacités électriques (dues à la double couche lipidique de la membrane cellulaire) et de résistances variables (dues aux canaux ioniques). Une interprétation simplifiée de cette vue porta à la formulation des modèles stochastiques à partir du modèle de Lapique et qui seront traités en détail dans le chapitre 2. Dans ce type de modèles, à chaque fois que le potentiel de membrane atteint un état particulier, le neurone produit un potentiel d'action, appelé *spike*. Cet état particulier

est souvent représenté par un seuil du potentiel de membrane: c'est une manière très pragmatique et pratique de traiter le problème mais ce n'est pas une description physiologique des processus biophysiques qui règlent la génération d'un spike.

Une autre approche du problème consiste en une approche phénoménologique qui est traitée computationellement par des modèles numériques digitaux, plutôt que analytiquement. Cette approche s'appuie sur des modèles neuronaux simplifiés appelés intégrateurs tout-ou-rien (en anglais: *integrate-and-fire*) est s'est développée à partir du travail de Mc Cullock et Pitts (1943) pour la simulation de réseaux neuronaux de grande taille.

Les deux approches ont chacune le pour et le contre et nous présentons dans cette thèse quelques idées qui pourraient représenter un compromis dans le sens que les formulations discrétisées des modèles analytiques pourraient être employées pour des simulations digitales intensives.

Connectivité neuronale

Le potentiel d'action est produit dans une zone particulière de la membrane cellulaire, la partie initiale de l'axone (cf. Fig. 0.1), et il est transmis dans toutes les branches de l'axone. Les points d'interaction entre deux neurones, les synapses, sont orientés de sorte que l'on différencie le neurone *présynaptique* (en anglais: le neurone *trigger*) et le neurone *postsynaptique* (en anglais: le neurone *follower*). Quand le potentiel d'action atteint la synapse, le neurone présynaptique libère un neurotransmetteur chimique qui traverse la fente synaptique et atteint la membrane du neurone postsynaptique où il se lie avec des récepteurs spécifiques. Il y a plusieurs genres de récepteurs (ionique, metabotropique, etc...) qui sont caractérisés par des temps d'activation allant de la milliseconde jusqu'à plusieurs secondes, par divers niveaux de plasticité et par divers effets de polarisation sur la membrane postsynaptique. L'effet de polarisation permet de distinguer les neurones en deux catégories principales: excitateur (si un courant de dépolarisation, EPSP, est produit) et inhibiteur (si un courant d'hyperpolarisation, IPSP, est produit).

Train de spikes

Ce travail aborde l'étude du système nerveux par le biais de modèles qui génèrent des trains de *spike*. Le train de *spike* est la sequence temporelle des potentiels d'action produits par une seule unité, habituellement un neurone. Les techniques expérimentales récentes ont évolué vers l'enregistrement de l'activité neuronale par des électrodes multiples permettant d'obtenir des séries temporelles multivariées correspondant aux trains de spike provenants de plusieurs cellules enregistrées simultanément. La répétition de ISI particuliers, au delà de la chance estimée du hasard, observée dans les trains de spike [**3**], [**6**], [**63**], [**64**] soulève plusieurs questions sur la signification que pourraient avoir de tels motifs temporels (en anglais: *pattern*) soit en rapport avec des motifs spécifiques d'activité neuronale au sein d'un réseau soit avec des propriétés intrinsèques propres à la membrane des cellules analysées.

Cadre du modèle adopté

Une sous-classe de pattern temporels, indiquée par les histogrammes multimodaux de la distribution des ISI, peut être étudiée en détail avec l'aide de modèles mathématiques de la dynamique neuronale. C'est l'approche que nous avons adopté dans cette étude. Le point de départ ont été les modèles stochastiques de saut-diffusion. Ce type de modèles décrit le potentiel de membrane à l'aide d'un processus de diffusion et de la somme de deux processus de point qui provoquent des sauts d'amplitude constante à des temps aléatoires discrets. En particulier nous avons étudié les deux modèles suivants (illustrés en détail dans le chapitre 2):

1. processus de diffusion de Wiener avec sauts;
2. processus de diffusion d'Ornstein Uhlenbeck avec sauts.

Structure de la dissertation

Le chapitre 1 introduit ce document, qui est divisé en deux sections. La première section (qui comprend les chapitres de 2 à 5) définit les fondements mathématiques des modèles neuromimétiques ainsi que les algorithmes utilisés pour leur simulation et pour les analyses des résultats computationnels. La deuxième section (chapitre 6) introduit et décrit en détail les résultats originaux obtenus dans la recherche purement mathématique des processus de

type “bridge”. Une conclusion générale (chapitre 7) reprend les résultats principaux et permet de comprendre les liens entre ces deux sections et les perspectives futures de ce travail.

Le chapitre 2 présente les équations mathématiques qui permettent d'analyser l'activité d'un neurone simplifié (appelé aussi neuromime) en fonction de certains paramètres caractéristiques. Ces paramètres décrivent l'évolution du potentiel membranaire du neurone à partir de deux hypothèses fondamentales. La première hypothèse est que le potentiel de membrane fluctue en suivant une trajectoire assimilée à celle d'un processus de diffusion. La deuxième hypothèse est qu'un certain nombre d'afférences neuronales influencent la fluctuation de cette trajectoire de manière très importante de sorte à lui imposer des sauts. La combinaison de ces deux hypothèses amène à la formulation du modèle “jump diffusion” (saut-diffusion). La variation du potentiel de membrane, dû à la combinaison de ces processus provoque la décharge du neurone au delà d'un certain seuil. La fin de ce chapitre est dédiée à l'interprétation biologique de ce modèle en particulier par rapport à la localisation proximale ou distale des afférences neuronales.

Le chapitre 3 introduit l'algorithme de simulation étudié pour approcher la discrétisation du processus “jump diffusion” (saut-diffusion) introduit dans le chapitre précédent. Cet algorithme se base sur les techniques connues pour simuler les processus de diffusion à partir de l'équation stochastique differentielle qu'ils vérifient. La présence des processus de saut et les problèmes liés à la surestimation du temps de premier passage requient l'utilisation de nouvelles techniques ici décrites.

Le chapitre 4 étudie le modèle neuronal de saut-diffusion dans lequel la diffusion est donnée par un processus de Wiener. Nous considérons les intervalles successifs (“ISI”) entre plusieurs décharges neuronales (“spike”). La distribution de ces intervalles est caractéristique de la dynamique neuronale. En fonction de plusieurs paramètres du processus de Wiener nous observons différentes classes de distributions ISI. Nous sommes particulièrment interessés aux distributions multimodales, qui peuvent être rapprochées à des observations expérimentales ou neurophysiologiques. Du point de vue du modèle nous analysons les conséquences des sauts dont la distribution des ISI suit une distribution exponentielle ou une distribution gaussienne inverse.

Le chapitre 5 étudie le modèle de saut-diffusion dans lequel la diffusion est donnée par un processus d'Ornstein Uhlenbeck. De manière similaire au chapitre precédent nous analysons

ici les effets des processus de sauts dont la distribution temporelle suit une distribution exponentielle ou une distribution gaussienne inverse. Dans les deux cas nous observons des distributions multimodales. Dans une marge restreinte de l'espace des paramètres nous observons la présence d'un phénomène nouveau, décrit ici pour la première fois. Il s'agit d'un phénomène de type résonnant ("resonant like") dû à la composition du processus diffusif et des processus de saut correspondant aux afférences excitatrices et afférences inhibitrices. Cette observation suggére que pour certaines intensités des processus de saut afférents ("bruit de fond") un neurone puisse participer à plusieurs assemblées de cellules ("cell assemblies").

Le chapitre 6 étudie les processus "bridge" associés à un processus de diffusion générique. L'analyse du temps de premier passage d'un processus de diffusion, approché par le temps de premier sortie d'un processus discretisé, laisse une ambiguïté sur la trajectoire exacte entre deux instants de la discrétisation. Le problème peut avoir de très graves conséquences dans l'évaluation de la solution. Pour résoudre ce problème on écrit l'équation stochastique differentielle satisfaite par le processus bridge. On propose deux méthodes alternatives pour trouver une version de la solution dans le cas bidimensionnel. Les méthodes présentées sont illustrées avec l'exemple du processus "Integrated Brownian Motion". Une généralisation de cette approche est indispensable à l'analyse des modèles neuronaux dans une simulation de réseaux de grand taille.

Le chapitre 7 rappelle le cheminement qui nous a permis de passer des modèles mathématiques simples aux modèles de plus en plus compliqués pour la simulation de la dynamique neuronale. Les principaux résultats obtenus sont rappelés sourtout à la lumière de leur interprétation neurobiologique: premièrement, l'observation qu'une afférence inhibitrice peut renforcer l'efficacité des afférences excitatrices sous certaines conditions; deuxièmement, l'observation des distributions ISI multimodales en l'absence d'afférences périodiques est particulièrment importante dans la perspective des synchronisations de l'activité cerebrale. Le dévelopement ultérieur des résultats de cette thèse, aussi bien dans le domaine des neurosciences computationelles que dans les applications informatiques, est décrit avec quelques exemples.

Conclusions

Nous avons développé ce travail dans deux directions principales. D'une part, nous avons étudié les modèles neuronaux stochastiques où le potentiel membranaire est décrit par un processus de saut-diffusion. Nous avons prouvé que, bien que simples, de tels modèles peuvent produire des dynamiques complexes et intéressantes. Nous avons concentré notre attention sur les propriétés des patterns de décharge d'un petit réseau composé par un neurone simple et par deux unités (cellules) afférentes. Les caractéristiques étudiées (plusieurs maxima dans les histogrammes d'ISIs, comportement résonnant, corrélations, rôle des afférences inhibitrices) permettent d'élargir la perspective et placer le micro réseau dans un environnement plus grand. D'autre part, d'un point de vue purement théorique, nous avons étudié les processus bridge multidimensionnels associés à un processus de diffusion.

L'étude du processus de diffusion de Wiener avec sauts est essentiellement préliminaire et nous a permis de présenter et focaliser les problèmes que nous avons développé plus en détail avec le processus d'Ornstein Uhlenbeck avec sauts. Les résultats que nous avons obtenu montrent que la superposition de sauts change considérablement la dynamique du potentiel membranaire. Quand les sauts sont distribués selon une distribution gaussienne inverse, les processus de saut forcent le potentiel membranaire á des fluctuations régulieres (cf. Fig. 5.3, panneaux *a*–*b*). Avec une distribution exponentielle des événements, les processus de saut n'ont aucune composante ni régulière ni oscillante (cf. Fig. 5.6, panneaux *a*–*b*), mais néanmoins la composition des sauts avec le processus de diffusion, pour certaines valeurs des paramètres, provoque des histogrammes d'ISI multimodaux. Ce résultat est particulièrement intéressant. En correspondance de chaque maximum de l'histogramme, la cellule a une probabilité plus élevée de décharger, de manière á ce que les latences des pics représentent des valeurs caractéristiques de la cellule. Ces temps peuvent représenter la "signature" de la participation d'un neurone à plusieurs circuits neuronaux. Ces temps pourraient être modulés par diverses conditions physiologiques et donner lieu à des phénomènes résonnants que nous avons mis en évidence avec les simulations.

Les autres résultats que nous avons obtenu sur l'étude du modèle neuromimétique mettent en évidence le rôle de l'inhibition dans le codage neuronal. En effet nous prouvons que l'inhibition peut aider à la transmission du signal excitateur (cf. Fig. 5.6, panneau *d*). Ce fait suggère que les cellules inhibitrices ne sont pas seulement impliquées dans la conservation

de l'équilibre entre excitation et inhibition mais qu'elles peuvent aussi également jouer un rôle important dans le traitement de l'information.

Nous avons aussi travaillé au traitement mathématique des processus bridge associés à un processus de diffusion. Nous avons obtenu des résultats purement théoriques que nous voudrions appliquer aux problèmes de simulation de temps de premier passage. Les algorithmes utilisés pour simuler le premier passage d'un processus stochastique (c'est à dire la formulation mathématique que nous avons adopté pour trouver les temps de décharge d'un neurone avec le potentiel membranaire modelé par un processus stochastique) permettent d'obtenir des approximations discrètes des trajectoires du processus simulé; à chaque étape les algorithmes évaluent si le nouveau point se trouve au delà du seuil. Cette procédure provoque le manque de détection des croisements possibles entre deux points successifs simulés. Nous ne pouvons pas observer de telles occurrences puisque nous ignorons la trajectoire exacte entre deux noeuds de l'approximation discrète de la trajectoire. Ainsi, l'erreur qui peut affecter l'estimation du temps de passage est très forte (cf. [**19**]). Notre travail suggère une correction de l'algorithme en ajoutant, à chaque étape, l'évaluation de la probabilité que le processus de bridge correspondant croise le seuil. Il faut noter que si nous traitons de grands réseaux de neurones et sommes intéressés par leur simulation, la présence d'une erreur à chaque évaluation du temps de premier passage pourrait provoquer une erreur importante sur l'activité d'une cellule qui se propagera et induirait une mauvaise interprétation des résultats.

Contents

List of Figures

CHAPTER 1

Introduction

Résumé Le chapitre 1 introduit le présent document divisé en deux sections: la première section (qui comprend les chapitres de 2 à 5) définit les fondementes mathématiques des modèles neuromimétiques ansi que les algorithmes utilisés pour leur simulation et pour les analyses des résultats computationnels. La seconde section (chapitre 6) introduit et décrit en détail les resultats originaux obtenus dans la recherche purement mathematique des processus de type "bridge". Une conclusion générale (chapitre 7) reprend les resultats et permet de comprendre les liens entre ces deux sections et les perspectives futures de ce travail.

Contents

To understand the functioning of brain functions is one of the major scientific challenges. Until the end of the nineteenth century, beginning of the twentieth, scientists were still not convinced that the brain tissue was made by cells. Santiago Ramón y Cajal, with his wonderful and massive histological work, convinced the scientific community that the brain was constituted by cells, the neurons, that are closed units interacting each other at specialized contacts called synapses. Nowadays we know that brain tissue is made up by two main kind of cells, the nervous cells, called neurons, and the neuroglial cells, called glia. Glia play important roles, not yet completely understood, which are not the goal of this study. The

unit we are interested in and that mainly deals with transmission of the *signal* is the neuron. When talking about nervous system often the term *signal* is used. But what is a *signal*?

1.1. Membrane dynamics

In the human nervous system it is possible to find about 10^{12} neurons, that exhibit extraordinary morphological and functional diversities. The number of different morphological classes of neurons in the vertebrate brain is estimated to be near 10^3. And that's a lot. However, as a starting point, we are going to describe a typical, and simplified, nerve cell (cf. Fig 1.1), with three basic components: the cell body, usually called *soma*, that is the part of the cell where the nucleus lies; the *dendrites* that branch several times and form treelike structures, the *dendritic tree*, and where, at specialized sites called *synapses*, the contact with other cells occur and the inputs arrive; the *axon* through which the output signal, *action potential*, propagates to reach other cells. There's a difference of potential between the inside and the outside of the neuronal cell, but what characterizes a neuron is that it is excitable, i.e. it can generate a neuronal signal both electrical and chemical. The electrical signal is carried through the membrane by ions, mainly sodium (Na^+), potassium (K^+), calcium (Ca^{2+}) and chloride (Cl^-). Even if the laws of the physics that regulate their movements are quite simple, the whole electrophysiological properties that characterize a neuronal cell are very complex.

The differential concentration of ions lead A. L. Hodgkin and A. F. Huxley [**24**] to formulate the first analytical description of the discharge of a nerve cell. They give differential equations for the membrane potential as a function of the conductances of the ions and get to the description of successive action potentials. Moreover the neuron membrane can be viewed as a series of capacitancies (due to the lipidic bilayer) and variable resistances (due to the ionic channels). A simplified interpretation of this view let to formulate the stochastic models that arise from the seminal Lapique's model and that are treated more in details in Chapter 2. With this kind of models, whenever the membrane dynamics reaches a particular state, the neuron generates an action potential, called *spike*. It is often considered that this particular state is represented by a threshold in the level of the membrane potential. This is a very pragmatic and practical way to treat the problem but it is not a physiological description of the biophysical processes that regulate the generation of a spike.

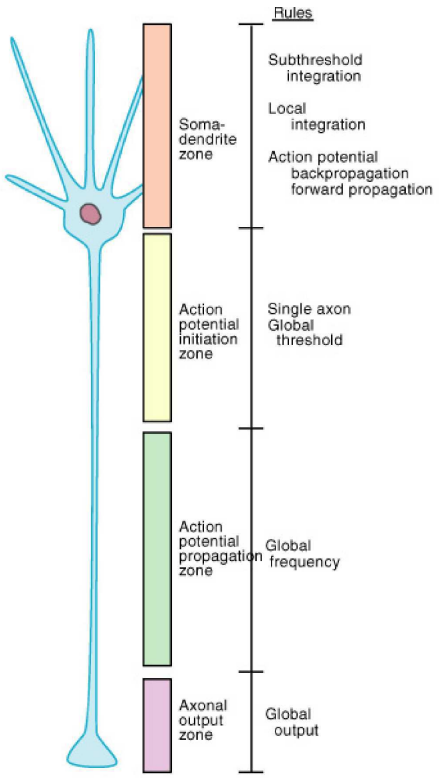

FIGURE 1.1. Schematic representation of a typical nerve cell.

Another approach to the problem is to consider simplified integrate and fire (IF) neurons, characterized by a phenomenological approach that is treated computationally rather that analytically. This alternative approach started to develop from the seminal work from Mc Cullock and Pitts (1943) and is the preferred approach (with refinements of the original formulation) of large scale neuronal networks simulations.

Both approaches have pros and cons and we introduce in this thesis some ideas that could represent a kind of compromise in the sense that discretized formulations of the analytical models might be used for computationally intensive simulations.

1.2. Neuronal connectivity

The action potential is generated in a particular area of the cell membrane, the initial part of the axon (cf. Fig. 1.1), and is transmitted throughout all the branches of the axon by means of electrotonic currents. The contact point between two neurons, called synapses, are oriented in the way that one neuron, the *trigger*, acts on another neuron, the *follower*. The trigger neuron is often called *pre-synaptic* neuron and the follower neuron is often calle *post-synaptic* neuron. When the action potential reaches the synapse the pre-synaptic neuron releases a chemical neurotransmitter that crosses the synaptic cleft and reaches the membrane of the post-synaptic terminal where it binds with receptors that are specific to the released neurotransmitter. There are many kind of receptors (ionic, metabotropic) which are characterized by time courses from milliseconds to seconds, by various levels of plasticity and by the polarizing effects on the post-synaptic membrane. This polarizing effect divides nerve cells into two main categories: excitatory (if a depolarizing current, EPSP, is generated after the neurotransmitter binds with the receptor) and inhibitory (if an hyperpolarizing current, IPSP, is generated after the neurotransmitter binds with the receptor).

1.3. Spike trains

We face the study of the nervous system, from a modelling point of view, through the analysis of the so called *spike trains*. The *spike train* is the time series corresponding to the times of occurrence of the action potentials generated by a single unit, that usually corresponds to one neuron. Experimental setups are often aimed to record single unit activity from one electrode such that the statistics of spike trains analysis is usually limited to descriptive values such as the mean firing rate. Most recent experimental techniques evolved towards the recording of neuronal activity by means of multiple electrodes that yields multivariate time series of simultaneously recorded spike trains. Particular attention has been given to recurrence of preferred time intervals above chance expectancy observed in spike trains under various experimental conditions [**3**], [**6**], [**63**], [**64**]. This observation raises several questions about the significance of such temporal patterns which may reflect either the existence of specific activity patterns sustained by specific neural connectivity or intrinsic activity patterns of the cell membrane. In order to understand the relation between the inputs to a neuron and the spike train it generates it would be idea to record from the axon of one neuron the

succession of action potential elicited by the cell and to know as well all the inputs incoming to the cell body. Actually this is not an achievable task and spike trains can be obtained from experimental extracellular recordings of neurons activity. But also from artificial neuromimes either modelled by mathematical functions or from electronic artifacts.

1.4. Framework of the adopted model

A subclass of temporal patterns, revealed by multimodal inter-spike interval (ISI) distribution histograms, can be investigated in detail by mathematical modelling of neuronal dynamics. This is the approach we adopted in the study here presented. The starting point has been the jump diffusion type stochastic models. Such kind of models describe the membrane potential in time as a diffusion process (continuous in time and in the state space) with the sum of two counting processes that provoke jumps of constant sizes at random times. In particular we studied the two following models (illustrated in detail in Chapter 2):

1. Wiener process with jumps, i.e. a stochastic perfect integrator with jumps model;
2. Ornstein Uhlenbeck process with jumps, i.e. a stochastic leaky integrator with jumps model.

The study of the first model (1) begins with paper [**20**]. There we investigated on the peculiarities of the model through the output frequency (f) and the coefficient of variation (CV), considered representative statistics of the ISI distribution. From this first work we realized that we could proceed in the analysis of the model considering histograms of the ISIs generated by the model. And successively with a generalization to the stochastic leaky integrator model with jumps (2).

1.5. Structure of the dissertation

The present manuscript is divided into two parts. The first one, called Neuro-modelling, collects the studies on neuronal models above mentioned. In Chapter 2 the stochastic perfect and leaky integrator with jumps models are introduced and discussed in their biological framework and Chapter 3 is devoted to the discussion of the simulation algorithms used to write the simulative programs. The results obtained on the first model are illustrated and discussed in Chapter 4. The results obtained on the second model are illustrated and discussed

in Chapter 5. The second part, called Bridge Processes, collects results on a mathematical investigation we developed and that has been inspired by simulative difficulties. This is a fully mathematical problem we faced while working on models. As will be mentioned in Chapters 3 and 6, bridge processes find a fundamental application in simulations of first passage times of diffusion processes through a threshold. The work presented in Chapter 6 is a study on multidimensional bridge processes through the construction of the stochastic differential equation (SDE) fulfilled by the bridge. Two methods to characterize the bridge process are given. The first one looks for time-space transformations that give a version of the solution of the SDE fulfilled by the bridge process, while the second one is based on a suitable conditioning of the solution of the second order SDE with Dirichlet type boundary condition appropriately written. The aim of this study is to develop methods to find analytical results on general bridge process with the intent to apply them to first passage time simulation problems. We give a final discussion and conclusion in Chapter 7. We decided not to write a Chapter dedicated to the mathematical background necessary to develop the works here presented. We will give references to the books and articles that hold the widenings and prerequisites useful for a better readability.

The work illustrated in this manuscript has been developed in strict collaboration between the Department of Mathematics of the University of Torino (Italy) and the Laboratoty of Preclinic Neurosciences of the University Joseph Fourier, Grenoble (France). The cooperation between mathematicians, electrophysiologists and computer scientists as well, lead to approach to the problem from different points of view. The exchange of knowledge and the necessity to find a common statement of the problem, made the study particularly stimulating. The biological interpretation of the models and the reinterpretation of the results in a suitable biological framework are the outcome of a in-depth study, a continuous dialog and edifying discussions between all the parts. And the analysis of the stochastic leaky integrator with jumps model illustrated in Chapter 5 is representative of this effort.

CHAPTER 2

Neuronal models

Résumé Le chapitre 2 présente les équations mathématiques qui permettent d'analyser l'activité d'un neurone simplifié (appelé aussi neuromime) en fonction de certains paramètres caractéristiques. Ces paramètres décrivent l'evolution du potentiel membranaire du neurone à partir de deux hypothèses fondamentales. La première hypothèse est que le potentiel de membrane fluctue en suivant une trajectoire assimilée à celle d'un processus de diffusion. La deuxième hypothèse est qu'un certain nombre d'afférences neuronales influencent la fluctuation de cette trajectoire de manière très importante de sorte à lui imposer des sauts. La combinaison de ces deux hypothèses amène à la formulation du modèle "jump diffusion" (saut-diffusion). La variation du potentiel de membrane, dû à la combinaison de ces processus provoque la décharge du neurone au delà d'un certain seuil. La fin de ce chapitre est dédiée à l'interprétation biologique de ce modèle en particulier par rapport à la localisation proximale ou distale des afférences neuronales.

Contents

In this Chapter we introduce the two neuronal models we studied during this Ph. D. thesis. After a brief introduction to stochastic neuro-models, we will derive the equations of the two jump-diffusion models we analyzed. Next we discuss the model from a biological point of view, to underline the motivations that lead us to study such kind of models and to introduce the framework in which the results will be interpreted and discussed.

2.1. Stochastic Neuronal models

There are two main classes of neuronal models. Deterministic models and stochastic models. The first ones make use of differential equations (with a threshold condition), or systems of differential equations, to describe the answer of the neuronal cell given an input current (cf. [**66**] and [**67**] for a review). For example, one of the simplest deterministic models is the so called Lapique model, that represents the single neuron as an equivalent electrical circuit made up by a resistance R and a capacitance C in parallel. Thus the evolution in time of the difference of potential across the cell membrane, $V = V(t)$, satisfies the following equation

$$C\frac{dV(t)}{dt} + \frac{V(t)}{R} = I(t), \tag{2.1.1}$$

where $t \geq 0$, $V(0) = v_0$, $I = I(t)$ is the input current and $V < S$ with S the threshold. An action potential is generated when $V(t)$ reaches the threshold S. Given the functional expression of the current I the sequence of times of occurrence of the spikes is uniquely determined and always the same. This is a deterministic model.

Beside this family of models, the stochastic models have been introduced. There are many and different reasons that may lead to conclude that deterministic models could be inadequate to describe the neuronal activity. First of all let us remark that usually the input current to the cell is not known. It is the (non linear) sum of all the inputs coming from the other neurons that have synapses on the dendritic tree of the considered cell. It seems difficult to give a mathematical expression of such a complex phenomena with a deterministic function of the time. We have to consider as well that many cells produce *spontaneous* activity, i.e. in absence of a stimulation coming from other cells. In the early '50s Fatt and Katz observed small random depolarizing potentials in the end-plate region of frog muscle fibers [**16**], [**14**]. They called them miniature end-plate potentials (m.e.p.p.) and showed that they occurred with "quantal" behavior, i.e. as multiples of a "quantum" quantity, and as random release of packets of neurotransmitters from synaptic vesicles, with mean rate from 1 to 100 per second. Moreover even in steady conditions small fluctuations in the membrane potential have been observed. These fluctuations are attributed to the continuous movement of the ions across the cellular membrane, due to the Brownian motion of the particles and to the changes in the conductance of the membrane as a consequence of the opening and closing of the ion channels. All the above described evidences of random behaviors cannot be properly described by a

deterministic mathematical function and drove mathematical neuronal modelling to make use of probabilistic tools. That is the membrane potential is described by means of a probabilistic law that allows to calculate the probability that at time t it attains a value in a given interval. In a stochastic model the membrane potential at time t, V_t, will be a random variable and the evolution of the membrane potential in time will be a stochastic process $V = \{V_t, t \geq 0\}$.

The mathematical description of the firing times of a neuron takes the form of a first passage time problem. That is we suppose that when the potential crosses a fixed threshold level above the resting potential the neuron fires and gives an output spike. After an action potential is emitted, the cell comes back to its resting potential and only when the membrane potential will reach again the threshold another action potential will be fired. The output of a neuron is the sequence of firings and the time of occurrence of an spike is given by the random variable

$$T = \inf\{t \geq 0 \mid V_t \geq S\}, \qquad V_0 < S, \tag{2.1.2}$$

that is the so called first passage time (FPT) of the stochastic process V across the threshold S. When the process V is not continuous in time, we will call T first exit time (FET) from the strip $(-\infty, S)$.

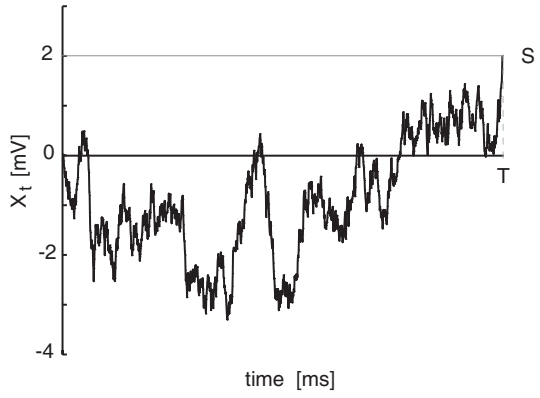

FIGURE 2.1. First passage time T (cf. eq. (2.1.2)) through the constant threshold S of a sample path of a general diffusion process $X = \{X_t,\ t \geq 0\}$.

2.1.1. The early models. The starting point of the stochastic modelling of neuronal cells is the assumption that the difference of potential across the cell membrane varies according to the inputs the cell receives from its dendritic tree. Thus an excitatory post synaptic

potential (EPSP) induces a depolarization of the membrane potential and an inhibitory post synaptic potential (IPSP) causes an hyperpolarization of the membrane potential. Moreover let us suppose that EPSPs and IPSPs arriving to the neuron are instantaneous and that they provoke a constant jump (positive or negative) in the membrane potential. So that EPSPs and IPSPs result completely determined by the time they occur and by the amplitude of the jump they provoke in the trajectory of the process describing the evolution of the membrane potential. It means that their occurrences can be described mathematically via two counting processes. Considering that the cell receives many inputs coming from all the neurons that have a synapse on its dendritic tree, the simplest equation we can write is the following:

$$V_t^{(1)} = V_{rest} + \sum_j V_t^{+,j} + \sum_k V_t^{+,k}, \tag{2.1.3}$$

where $V^{(1)} = \{V_t^{(1)}, t \geq 0\}$, the membrane potential at time t, is a stochastic process continuous in time, V_{rest} is the resting potential, $V^{+,j} = \{V_t^{+,j}, t \geq 0\}$ and $V^{-,k} = \{V_t^{-,k}, t \geq 0\}$ $\forall j, k \in \mathbb{N}$ are counting processes that at time t give the number of events (EPSPs and IPSPs respectively) occurred in the depolarization and hyperpolarization procesesses. Note that, for the sake of simplicity, in eq. (2.1.3) the amplitude of the jumps in the trajectory of the membrane potential due to incoming EPSPs and IPSPs is considered unitary.

If the number of superimposed counting processes is sufficiently large, use can be made of results (cf. [**54**] and [**29**]) stating that, under suitable assumptions (like the stationarity of the superimposed sequences and bounded spike rate of the pooled sequence), it is possible to approximate the sum of such processes with a Poisson process. That is it is possible to approximate process $V^{(1)}$ with process $V^{(2)} = \{V_t^{(2)}, t \geq 0\}$ given by

$$V_t^{(2)} = V_{rest} + a_+ N_t^+ + a_- N_t^-, \tag{2.1.4}$$

where the processes $N^+ = \{N_t^+, t \geq 0\}$, $N^- = \{N_t^-, t \geq 0\}$ are two independent Poisson processes of parameters λ^+ and λ^- respectively and with $N_0^+ = N_0^- = 0$ that approximate the sums in eq. (2.1.3) and $a_+ > 0$ and $a_- < 0$ are the amplitudes of the change of the membrane potential due to an incoming EPSP or IPSP respectively.

If the following hypothesis are introduced, $a_+, a_- \to 0$ and $\lambda^+, \lambda^- \to \infty$ such that

$$\begin{aligned} a_+\lambda^+ + a_-\lambda^- &\to \mu \\ a_+^2\lambda^+ + a_-^2\lambda^- &\to \sigma^2 \end{aligned} \tag{2.1.5}$$

eq. (2.1.4) can be approximated with a Wiener process with drift (cf. [**67**]). That is process $V^{(2)}$ can be approximated by the diffusion process $V^B = \{V_t^B, t \geq 0\}$ solution of the following stochastic differential equation (SDE)

$$\begin{aligned} dV_t^B &= \mu dt + \sigma dW_t \\ V_0^B &= V_{rest}, \end{aligned} \tag{2.1.6}$$

where μ is the drift coefficient, $\sigma > 0$ is the diffusion coefficient and $W = \{W_t, t \geq 0\}$ is a standard Brownian motion. Process V^B is continuous in time with trajectories that are continuous functions of the time, thus possible to study analytically, since the difference equations that arise when handling discrete time process are here substituted with differential equations that are easier to solve. This model has been introduced at first by Gerstein and Mandelbrot in [**18**]. They studied the statistical properties of spontaneously occurring spike trains from single neurons, such as the inter-spike interval (ISI) distribution and the joint distribution of successive ISIs, with the intention to give a mathematical model with first passage time distributions well fitting with recorded data. They introduced the random walk model, i.e. a standard Brownian motion. To obtain a better agreement between data and model they corrected it with the random walk model with drift, i.e. the Brownian motion with drift given by eq. (2.1.6). This way they obtained a good fit of a wide variety of neurophysiological observations. The main advantage gained using the random walk model with drift is that the distribution of the first passage time through a constant threshold is analytically calculated. Named g the probability density function of the random variable first passage time (2.1.2) of the process (2.1.6) through the constant threshold S, it is given by

$$g(x; a, b) = \sqrt{\frac{b}{2\pi}}\, x^{-3/2} \exp\left[-\frac{b(x-a)^2}{2a^2 x}\right], \quad x > 0, \tag{2.1.7}$$

where $a = |S - V_{rest}|/\mu$ and $b = (S - V_{rest})^2/\sigma^2$, i.e. it is Inverse Gaussian distributed $IG(a, b)$. However the model can be improved. As Gerstein and Mandelbrot remarked in their paper, this model is "a gross oversimplification that does not take into account the complex geometry of the neuron membrane and the complicated distribution of synaptic knobs [**45**]". Such complexity can be partially recovered in the discrete model (2.1.4) considering that both EPSPs and IPSPs incoming to the cell provoke different jumps in the membrane potential according to the strength of the synapse connecting the two neurons, so that the membrane

potential is described by the process $V^{(3)} = \{V_t^{(3)}, t \geq 0\}$ defined by

$$V_t^{(3)} = V_{rest} + \sum_j a_+^j N_t^{+,j} + \sum_k a_-^k N_t^{-,k}, \tag{2.1.8}$$

where $N^{+,j}$ and $N^{-,j}$, $\forall j,k \in \mathbb{N}$ are independent Poisson process with parameters $\lambda^{+,j}$ and $\lambda^{-,k}$ respectively and a_+^j and a_-^k, $\forall j,k \in \mathbb{N}$ are the amplitudes of the jumps in the membrane potential due to EPSPs and IPSPs reaching the cell.

In 1965 Stein [**62**] introduced a further improvement in the discrete model of a single neuron (2.1.8), saying that the underthreshold membrane potential could be modelled with the stochastic process $V^{(4)} = \{V_t^{(4)}, t \geq 0\}$ given by

$$\begin{aligned} dV_t^{(4)} &= -\frac{1}{\theta} V_t^{(4)} dt + \sum_j a_+^j dN_t^{+,j} + \sum_k a_-^k dN_t^{-,k} \\ V_0^{(4)} &= V_{rest} \end{aligned} \tag{2.1.9}$$

where $N^{+,j}$, $N^{-,j}$, a_+^j and a_-^k are as in equation (2.1.8) and θ is the so called time constant of the membrane. This model assumes that in between two successive inputs, the membrane potential decays exponentially to its resting value. That is an electrophysiological property of the neuron observed in recorded data [**15**] due to the resistive and capacitative properties of the biological membrane (cf. eq. (2.1.1)). Model (2.1.9) is not easy to handle analytically. Methods to approximate such equation with a diffusion process have been proposed by Kallianpur, Capocelli and Ricciardi and Lánský [**25**], [**26**], [**49**], [**46**], [**12**] and [**33**]. They state that for $a_+^j, a_-^k \to 0$ and $\lambda^{+,j}, \lambda^{-,k} \to \infty$ such that

$$\begin{aligned} \sum_j a_+^j \lambda^{+,j} + \sum_k a_-^k \lambda^{-,k} &\to \mu \\ \sum_j (a_+^j)^2 \lambda^{+,j} + \sum_k (a_-^k)^2 \lambda^{-,k} &\to \sigma^2 \end{aligned} \tag{2.1.10}$$

the process $V^{(4)}$ solution of the SDE (2.1.9) converges in distribution to the process $V^{OU} = \{V_t^{OU}, t \geq 0\}$ solution of the following SDE

$$\begin{aligned} dV_t^{OU} &= \left(-\frac{1}{\theta} V_t^{OU} + \mu\right) dt + \sigma dW_t \\ V_0^{OU} &= V_{rest} \end{aligned} \tag{2.1.11}$$

where $W = \{W_t, t \geq 0\}$ is a standard Brownian motion, μ and $\sigma > 0$ are the infinitesimal moments of the process and θ keeps the same meaning as in eq. (2.1.9). Process V^{OU} is the so called Ornstein Uhlenbeck (OU) process, a Gaussian Markov diffusion process.

2.1.2. Jump diffusion models. Models (2.1.6) and (2.1.11) obtained as continuous approximations of discrete models (2.1.4) and (2.1.9) allow, from a mathematical point of view, to obtain more analytical results in their analysis. But it is worth to remember that their discrete versions better describe, from a biological point of view, the neurophysiological characteristics of the neuron. In particular Stein's model (2.1.9) is accepted as a good description of the membrane potential behavior. It is important not to forget that the procedure to approximate the discrete model with the continuous one needs the hypothesis (2.1.5) and (2.1.10). That is it is necessary to hypothesize that the frequencies of the incoming inputs tends to infinity, i.e. at least very very big, and that the amplitudes of the EPSPs and IPSPs go to zero, i.e. at least very very small. Since the involved quantities have a direct biological meaning, we cannot ignore that conditions (2.1.5) and (2.1.10) may have a consequence in the validity and goodness of the model itself. To reach a better physiological likelihood mixed models have been introduced, i.e. models with a part that is continuous and a part that is discrete and that are called jump diffusion models [**40**].

Let us consider Stein's model (2.1.9) and let us separate the synaptic inputs in two groups. The first one is referred to as the *strong* inputs, i.e. the inputs with strong impact on the membrane potential (a_+ and a_-) interpreted as a strong synaptic weight. Let us distinguish them from all the *weak* inputs, i.e. with weak synaptic weight, labelled with superscript WW. Then isolating the strong inputs from the sum of the weak inputs eq. (2.1.9) can be rewritten as

$$\begin{aligned} dV_t^{(5)} &= -\frac{1}{\theta}V_t^{(5)}dt + \sum_j a_+^{WW,j} dN_t^{+,WW,j} + \sum_k a_-^{WW,k} dN_t^{-,WW,k} + a_+ dN_t^+ + a_- dN_t^- \\ V_0^{(5)} &= V_{rest}, \end{aligned} \tag{2.1.12}$$

where $\forall j, k \in \mathbb{N}$, $N^{+,WW,j}$ and $N^{-,WW,k}$ are independent homogeneous Poisson processes of intensities $\lambda_{WW}^{-,j}$ and $\lambda_{WW}^{+,k}$ respectively. Applying the procedure we explained for eq. (2.1.9)

with

$$\begin{aligned} \sum_j a_+^{WW,j}\lambda_{WW}^{+,j} + \sum_k a_-^{WW,k}\lambda_{WW}^{-,k} &\to \mu \\ \sum_j (a_+^{WW,j})^2\lambda_{WW}^{+,j} + \sum_k (a_-^{WW,k})^2\lambda_{WW}^{-,k} &\to \sigma^2 \end{aligned} \tag{2.1.13}$$

we obtain the following equation describing the membrane potential evolution according to the jump diffusion process $V^{OUJ} = \{V_t^{OUJ}, t \geq 0\}$

$$\begin{aligned} dV_t^{OUJ} &= \left(-\frac{1}{\theta}V_t^{OUJ} + \mu\right)dt + \sigma dW_t + a_+ dN_t^+ + a_- dN_t^- \\ V_0^{OUJ} &= V_{rest}, \end{aligned} \tag{2.1.14}$$

where μ and $\sigma > 0$ are the infinitesimal moments called drift (with no direct biological interpretation) and diffusion coefficient (the intensity of the Brownian motion), $a_+ > 0$ and $a_- < 0$ are the amplitudes of the jumps in the membrane potential due to strong excitatory (inhibitory) post-synaptic potential reaching the cell, N^+ and N^- are independent homogeneous Poisson processes with $N_0^+ = N_0^- = 0$ and θ keeps the same meaning as in eq. (2.1.9). Eq. (2.1.14) can be rewritten in integral form as

$$V_t^{OUJ} = V_{rest} + \int_0^t \left(-\frac{1}{\theta}V_s^{OUJ} + \mu\right)ds + \sigma W_t + a_+ N_t^+ + a_- N_t^-. \tag{2.1.15}$$

The process V^{OUJ} is a jump diffusion process whose trajectories present discontinuities at discrete times (determined by processes N^+ and N^-) and evolve as trajectories of an Ornstein Uhlenbeck process in the time intervals where the process is continuous.

It is possible to apply the same arguments to model (2.1.8) as well, that corresponds to Stein's model with $\theta \to \infty$. Separating strong inputs from weak inputs and approximating with a Wiener process with drift we obtain the following equation for the membrane potential $V^{WJ} = \{V_t^{WJ}, t \geq 0\}$

$$\begin{aligned} dV_t^{WJ} &= \mu dt + \sigma dW_t + a_+ dN_t^+ + a_- dN_t^- \\ V_0^{WJ} &= V_{rest}, \end{aligned} \tag{2.1.16}$$

where μ and $\sigma > 0$ are the drift and the diffusion coefficient, $a_+ > 0$, $a_- < 0$, N^+ and N^- are as in eq. (2.1.14). Written in integral form eq. (2.1.16) becomes

$$V_t^{WJ} = V_{rest} + \mu t + \sigma W_t + a_+ N_t^+ + a_- N_t^-. \tag{2.1.17}$$

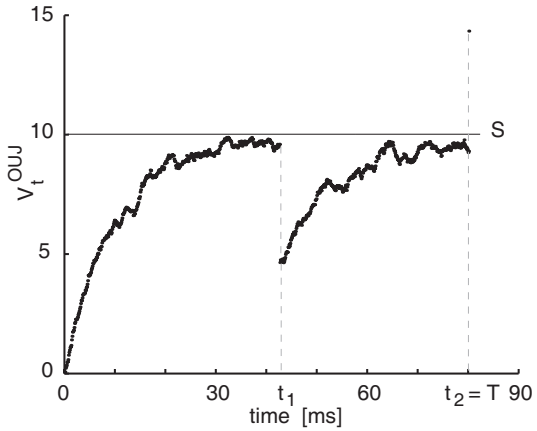

FIGURE 2.2. First passage time through the constant threshold $S = 10$ mV of a sample path of the jump diffusion process V_t^{OUJ} in (2.1.15) with $\mu = 0.98$ mVms^{-1}, $\theta = 10$ ms, $\sigma^2 = 0.05$ mV^{2}ms^{-1}, $\lambda^+ = 30$ and $\lambda^- = 20$ [ev/s], $a_+ = -a_- = 5$ mV. Here t_1 and t_2 are times of occurrence of a downward jump (in the process N^-) and of an upward jump (in the process N^+) respectively and T is the first passage time defined in (2.1.2).

Process V^{WJ} is a jump diffusion process whose trajectories show discontinuities at discrete times (determined by processes N^+ and N^-) and evolve as trajectories of a Wiener process with drift in the points of continuity.

We will refer to such models as OU process with jumps (2.1.14) and Wiener process with jumps (2.1.16), naming "diffusive" the continuous parts of the processes and "discrete" the jump processes. Furthermore we will consider as well some generalizations of equation (2.1.17). For both the models we will examine the following modification. Besides the instance with processes N^+ and N^- that are Poisson processes, we will consider that N^+ and N^- are counting processes with inter events distributed according to IG distributions with parameters $(|S_+|/\mu^+, S_+^2/\sigma_+^2)$ and $(|S_-|/\mu^-, S_-^2/\sigma_-^2)$ respectively. This way the jump processes may be interpreted as coming from pools of neurons firing following an IG distribution (2.1.7), i.e. whose membrane potential is modelled with a random walk model (2.1.6) as pointed out in the previous Section. The further generalization we will study only involves model (2.1.14). After an action potential is generated the membrane potential is reset to its resting state value V_{rest}, i.e. the diffusion process V^{OU} and the two counting processes N^+ and N^- are all reset to their initial values $V_0^{OU} = V_{rest}$ and $N_0^+ = N_0^- = 0$. The sequence $(T_i)_{i=1}^{+\infty}$ of successive first exit times (2.1.2) is a renewal process and n repeated simulations of the

FETs $T_1, T_2, ..., T_n$ give us a sample of n independent identically distributed random variables representing the ISI of a single neuron. However, we consider as well the case where after a spike the counting processes N^+ and N^- are not reset to their initial values $N_0^+ = N_0^- = 0$. Let us define T_k the k-th FET from the strip. In order to evaluate the next FET, T_{k+1}, the jump processes are set to the values $N_0^+ = N_{T_k}^+$ and $N_0^- = N_{T_k}^-$ while the diffusion process is reset to its initial value $V_0^{OU} = V_{rest}$. In this case n repeated simulations of the FETs $T_1, T_2, ..., T_n$ give us a discrete time serie that is no longer a renewal process.

To summarize, in the next Chapters we will explain the results we obtained analyzing the following models:

- Wiener process with jumps (2.1.16):
  - N^+ and N^- Poisson processes
  - N^+ and N^- with inter events IG distributed
- Ornstein Uhlenbeck process with jumps (2.1.14):
  - with reset to $V_0^{OU} = V_{rest}$ and $N_0^+ = N_0^- = 0$:
    - N^+ and N^- Poisson processes
    - N^+ and N^- with inter events IG distributed
  - with reset to $V_0^{OU} = V_{rest}$ and $N_0^+ = N_{T_k}^+$ and $N_0^- = N_{T_k}^-$:
    - N^+ and N^- Poisson processes
    - N^+ and N^- with inter events IG distributed

2.2. Biological interpretation of the models

Models (2.1.16) and (2.1.14) describe the evolution in time of the membrane potential (the difference of potential between inside and outside the cell body) by means of two jump diffusion processes. That is, they include a diffusive part of the equation that defines a diffusion process continuous in time with continuous state space and a discrete part that is the sum of two counting processes (N_t^+ and N_t^-), that provokes discontinuities (i.e. jumps) in the trajectories of the process V_t at randomly distributed times.

In this Section we try to give the motivations that lead us to study such models in order to introduce the biological framework in which we will discuss the results. We would like to point out that model (2.1.16) may be considered as a particular case of model (2.1.14),

i.e. for $\theta \to +\infty$. It has been for us a "simplification" and a "preliminary" study to better approach to model (2.1.14). From a modelling point of view as well it has been recognized that the Wiener process with drift, the so called random walk model with drift, is an excessive simplification of neurophysiological characteristics of neurons. So that the starting point should be Stein's model (2.1.9), or at least its continuous counterpart, the OU process (2.1.11). But we believe that the main limitation of such model is in the unrealistic assumptions that have to be done to substitute eq. (2.1.9) with eq. (2.1.11). So we introduce model (2.1.14) that considers both EPSPs and IPSPs that may have a stronger impact on the membrane potential and a frequency that falls into biological ranges. The inputs we call *weak* are summed together and approximated with the diffusion process (2.1.11), and the ones we call *strong* that cannot be approximated because they not fulfil conditions (2.1.13), are treated separately by means of the two counting processes N_t^+ and N_t^-.

From a biological point of view the question is: where do strong inputs come from? To explain the phenomenon let us treat separately EPSPs from IPSPs.

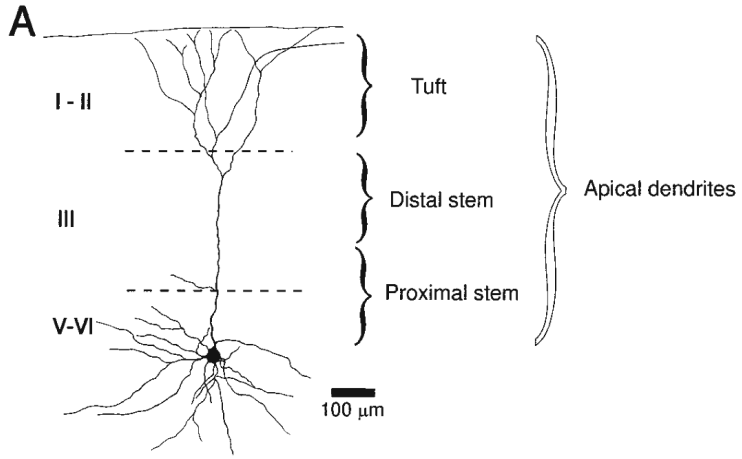

FIGURE 2.3. Distal and proximal apical dendritic stem regions. (Modified from [**55**]).

The strong IPSPs introduced in the model are suggested by the so called shunting inhibition phenomenon (cf. [**56**] and [**65**]). Such term refers to the activation of an inhibitory synapse that prevents coincident EPSPs to depolarize the trigger zone of the axon. As a consequence of such temporal summation of the two kind of stimuli, the neuron does not generate

an action potential. Such phenomenon is included into the model by means of strong IPSPs provoking an abrupt hyperpolarization of the membrane potential and a consequent inability of the cell to elicit an action potential.

As far as excitation is concerned, the stimuli we introduce into the model represent EPSPs coming to the soma through particularly strong synapses. About the reason of such strength we restrict here ourselves to only sketch the phenomena that can give as a result more effective synapses. Actually, how it happens that some stimuli are stronger than others, it's a question that still has not a unique answer. Even more, the way a nerve cell transforms thousands of incoming synaptic inputs into a specific pattern of action potential output still is a non answered question. Possible biological explanations of such differences in synaptic strength have been searched in more directions and we sketch here some of them. First of all more realistic assumptions should separate the inputs occurring on distal dendrites, which represent the vast majority, from the inputs on proximal dendrites or on the cell body. Distal inputs occur on membrane sites characterized by passive conductance properties well described by the cable theory of dendrites (cf. [**45**] and [**51**]). According to this theory the farther from the cell body the more attenuated and slowed down will be the effects of the post-synaptic potentials. Proximal inputs occur on membrane sites characterized by active conductance properties. Non linear active membrane properties of proximal excitatory inputs may produce a strong depolarization of the cell membrane either after a single large EPSP or after temporal summation (the non linear sum of two or more EPSPs very near in time) or spatial summation (the nonlinear sum of EPSPs very near in space) [**36**], [**69**]. In the present study the distal inputs are labelled *weak* and approximated by the diffusion process (2.1.11). The proximal inputs are labelled *strong*, described by the counting processes N_t^+ and N_t^- at frequencies that fall in the biological ranges. But recent experiments and multi-site patch-clamp recordings from the soma and the apical dendrites of pyramidal neurons let emerge contrasting results. In [**37**] it is shown that in CA1 hippocampal pyramidal neurons the average somatic amplitude of EPSPs is independent from the apical dendrite site of generation, whereas in [**68**] it is said that in layer 5 neocortical pyramidal neurons the average somatic amplitude of EPSPs decreases as the synapse location in the apical dendritic tree is farther. So that the question remains, in a certain sense, open and feed a heated scientific debate [**34**].

Furthermore we would like to recall the Hebbian learning theories that suggest that the strength of a synapse is the result of the "history" of the synapse, how much and in coincidence of which stimuli it has been activated. In particular Hebb suggested that synapses in the brain become stronger if there is a correlation between the presynaptic and postsynaptic activities [**23**]. He spoke of strengthening synapses in which the presynaptic activity slightly preceded the postsynaptic activity. In accordance with those theories, the strong EPSP incoming to the cell can be attributed to a synapse that, independently on its position in the dendritic tree, increased its strength as a consequence of a learning phenomenon.

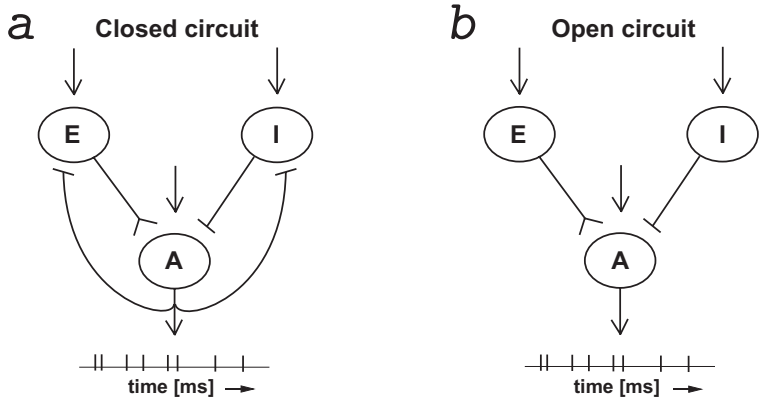

FIGURE 2.4. The model (2.1.14) describes a small networks of neurons with a reference unit A that receives a pool of excitatory inputs from unit E and inhibitory inputs from unit I. (**a**) The circuit is *closed*, characterized by a feedback of A on E and I that provokes a reset of the diffusion process and of the two jump process after each spike of unit A. (**b**) The circuit is *open*, with no reset of the two jump processes.

Figure 2.4 illustrates the model assuming the strong inputs project on a reference unit A from pools of excitatory E and inhibitory I units. Notice that in model (2.1.14) the process V^{OUJ} is reset to its initial value V_{rest} after each crossing of the threshold S. It means that also the processes N_t^+ and N_t^- are reset to their initial values N_0^+ and N_0^- after each FET. Such hypothesis is very helpful from a mathematical point of view because the sequence of FET generated by process V^{OUJ} is a renewal process, but it implies that neuron A has an inhibitory feedback on units E and I and makes the circuit *closed* (cf. Fig. 2.4a). The removal of the inhibitory feedback from unit A to units E and I implies that after each crossing of the threshold, processes N^+ and N^- are not reset to their initial values and only the diffusion process (2.1.11) is reset (cf. Fig. 2.4*b*). Under such assumptions the modelled

circuit can be considered an *open* circuit, but for a mathematical treatment of the serie of the FETs generated by the process V^{OUJ} it is necessary to remember that it is no more a renewal process.

To conclude we would like to remark that we are interested in the impact of strong postsynaptic potentials on the generation of action potentials. That is to say that we believe that there exists biological evidence of different synaptic weights and we would like to study how the sequence of action potentials elicited by the cell is affected by that. As long as the biological mechanism that leads to the generation of such strength, we consider the debate open.

CHAPTER 3

Simulation Algorithms

Résumé Le chapitre 3 introduit l'algorithme de simulation étudié pour approcher la discrétisation du processus "jump diffusion" (saut-diffusion) introduit dans le chapitre précédent. Cet algorithme se base sur les techniques connues pour simuler les processus de diffusion à partir de l'équation stochastique differentielle qu'ils vérifient. La présence des processus de saut et les problèmes liés à la surestimation du temps de premier passage requient l'utilisation de nouvelles techniques ici décrites.

Contents

In this Chapter the simulation algorithm employed to calculate the trajectories of the jump-diffusion processes, solutions of eq. (2.1.16) and (2.1.14), is introduced. The estimation of the random variable FET from the strip $(-\infty, S)$ of such processes is based on a suitable discrete time approximation of the trajectories, obtained modifying the techniques introduced in [**30**] and adapting the method proposed in [**19**] to jump diffusion processes. For an in-depth review on first passage problems approached from a theoretical point of view, we address the reader to the paper [**50**] and references quoted therein. And for an outline on numerical and algorithmic approach to first passage problems we refer to [**48**] and references quoted therein.

3.1. The algorithm

The simulation of the FET from a strip of a jump diffusion process introduces two main difficulties.

The first one is due to the presence of the jump processes. Indeed it is necessary to modify the techniques proposed in [**30**] for the solution of a stochastic differential equation (a diffusion process) through a discrete time approximation. Let us suppose that the process to simulate $Y = \{Y_t, t \geq t_0\}$ is the solution of the generic SDE

$$\begin{aligned} dY_t &= a(t, Y_t)dt + b(t, Y_t)dWt \\ Y_{t_0} &= y_0, \end{aligned} \tag{3.1.1}$$

where $W = \{W_t, t \geq t_0\}$ is a standard Wiener process and the coefficients a and b fulfil the conditions necessary to the existence and uniqueness of a solution of the SDE [**7**]. Given the time discretization $t_0 < t_1 < t_2 < ... < t_N = T$ of the time interval $[t_0, T]$, the approximation of process Y, that we name $\tilde{Y} = \{\tilde{Y}_t, t \geq t_0\}$, is calculated on the times of the discretization $(t_i)_{i=0}^N$ according to different schemes (cf. [**30**]), obtained as truncations of the stochastic Taylor expansion of the process Y. If the noise term is additive, a good approximation of the solution is obtained even with a truncation of the Taylor expansion at the first order. So that in the case of a Wiener process with drift (2.1.6) the discrete time approximation $\tilde{Y}^W$ on the times $(t_i)_{i=0}^N$ is given by

$$\tilde{Y}^W_{t_{i+1}} = \tilde{Y}^W_{t_i} + \mu(t_{i+1} - t_i) + \sigma\sqrt{t_{i+1} - t_i}Z_i \tag{3.1.2}$$

where Z_i are independent identically distributed Standard Normal random variables, and μ and σ are as in eq. (2.1.6). This is the so called Euler scheme. While if considering an OU process (2.1.11), the discrete time approximation $\tilde{Y}^{OU}$ on the times $(t_i)_{i=0}^N$ is given by

$$\tilde{Y}^{OU}_{t_{i+1}} = \tilde{Y}^{OU}_{t_i} + \left(\frac{1}{\theta}\tilde{Y}^{OU}_{t_i} + \mu\right)(t_{i+1} - t_i) + \sigma\sqrt{t_{i+1} - t_i}Z_i \tag{3.1.3}$$

where Z_i are as in eq. (3.1.2) and μ, θ, σ are as in eq. (2.1.11). Those techniques are proved to be efficient even for non constant and random step sizes of the time discretization $(t_i)_{i=0}^N$. So that to include the jump processes, we proceed as follows: each time the occurrence of a jump falls in between a discretization interval $[t_i, t_{i+1}]$, in the i-th step of the algorithm the new node t_{i+1} it is replaced with the time of the jump and the approximation $\tilde{Y}_{t_{i+1}}$ is calculated. Finally the jump amplitude is summed to the simulated value $\tilde{Y}_{t_{i+1}}$.

The second problem that emerges is about the estimation of the FET. Indeed at each step it is checked whether the approximated value overcome the threshold, i.e. if $\tilde{Y}_{t_n} \geq S$. This way, probable crossing occurring at times in between two nodes t_i and t_{i+1} of the time

discretization are not detected. As a consequence the FET is systematically overestimated. To overcome this difficulty let us consider the approach to the problem illustrated in [**19**]. Given a diffusion process $Y = \{Y_t; t \geq t_0\}$ with in $Y_{t_0} = y_0$ we can associate a corresponding bridge process $\hat{Y}_t = \{\hat{Y}_t; t \in [t_0, t_1]\}$ (also called tied down process [**28**] or pinned process [**8**]) defined as the process Y_t conditioned on the event $\{Y_{t_1} = y_1\}$. At each step of the algorithm, the probability $\hat{p}$ that the tied down process $\hat{Y}$ originated in $(t_i, \tilde{Y}_{t_i})$ and constrained to assume the value $(t_{i+1}, \tilde{Y}_{t_{i+1}})$ exits from the strip, is evaluated and when a simulated uniform random variable falls in the interval $[0, \hat{p}]$ it is assumed that the bridge process exits from the strip. In the case of a Wiener process with drift the probability that the bridge process originated in $(t_i, \tilde{Y}_{t_i})$ and constrained to assume the value $(t_{i+1}, \tilde{Y}_{t_{i+1}})$ crosses the threshold is given by

$$\hat{p}^W = \exp\left[-\frac{2(S^2 - S\tilde{Y}^W_{t_i} - S\tilde{Y}^W_{t_{i+1}} + \tilde{Y}^W_{t_i}\tilde{Y}^W_{t_{i+1}})}{\sigma^2(t_{i+1} - t_i)}\right] \tag{3.1.4}$$

and directly evaluated. When considering an OU process, we can evaluate $\hat{p}^{OU}$ by means of the approximation proposed in [**19**]. Note that the presence of jumps does not introduce new difficulties in the correction of the simulative procedure via bridge processes. Indeed the algorithm is built such that times of occurrence of the jumps are nodes of the time discretization and in between two nodes the process has no discontinuities.

We now illustrate in details the algorithm procedure. Let us denote with $\tilde{Y}_{t_i}$ the simulated solution of the SDEs (2.1.6) or (2.1.11), i.e. the diffusion process, and $\tilde{V}_{t_i}$ the simulated solution of eq. (2.1.16) or (2.1.14), i.e. completed with the jump processes. The maximum step h of the time discretization is fixed and t^+ and t^-, times of occurrence of events in the processes N^+ and N^-, are generated.

The iterative stepwise procedure of the algorithm is described as follows.

Step 1. Set $t_{i+1} = \min\{t_i + h, t^+, t^-\}$;

Step 2. Evaluate the approximated solution of SDEs (2.1.6) or (2.1.11) in t_{i+1} according to (3.1.2) or (3.1.3) respectively;

Step 3. **IF** $(\tilde{Y}_{t_{i+1}} \geq S)$ **GOTO Step 10** ;

Step 4. Generate a pseudo-random number U uniformly distributed in $[0, 1]$ and compare it with the probability $\hat{p}$ that the corresponding tied down process constrained in $(t_i, \tilde{Y}_{t_i})$ and $(t_{i+1}, \tilde{Y}_{t_{i+1}})$ crosses the boundary S ;

Step 5. IF $(U < \hat{p})$ **GOTO Step 10** ;

Step 6. IF $(t_{i+1} = t_i + h)$ **THEN** {

$\tilde{V}_{t_{i+1}} = \tilde{Y}_{t_{i+1}}$;

$t_i = t_{i+1}$;

GOTO Step 1 ; }

Step 7. IF $(t_{i+1} = t^+)$ **THEN** {

$\tilde{V}_{t_{i+1}} = \tilde{Y}_{t_{i+1}} + a_+$;

Generate a new inter-time t^+_{new} between two events in the process N^+_t ;

$t^+ = t^+ + t^+_{new}$; }

Step 8. IF $(t_{i+1} = t^-)$ **THEN** {

$\tilde{V}_{t_{i+1}} = \tilde{Y}_{t_{i+1}} + a_-$;

Generate a new inter- time t^-_{new} between two events in the process N^-_t ;

$t^- = t^- + t^-_{new}$; }

Step 9. IF $(\tilde{Y}_{t_{i+1}} < S)$ **THEN** {

$t_i = t_{i+1}$;

GOTO Step 1 ; }

Step 10. The algorithm **stops** and returns the first exit time (FET) $T = t_{i+1}$.

The generation of Inverse Gaussian distributed pseudo-random numbers is performed following the method described in [**38**] that makes use of transformations of random variables with multiple roots. While the generation of Exponentially distributed pseudo-random numbers is trivial thanks to the classic method of inverse transformation that produces exponentially distributed inter-times. The algorithm has been written in C language and the simulations run on Pentium III personal computers.

Notice that the proposed algorithm works for the simulation of the trajectories of any jump diffusion process but difficulties can arise in evaluating $\hat{p}$. In non additive noise instances it is recommended at **Step 2** to use a discrete time approximation of the diffusion process Y of higher strong convergence order in substitution of the Euler scheme [**30**].

Part 1

Neuro-modelling

CHAPTER 4

A Wiener process with jumps as a simple neuronal model

Résumé Le chapitre 4 étudie le modèle neuronal de saut-diffusion dans lequel la diffusion est donnée par un processus de Wiener. Nous considérons les intervalles successifs ("ISI") entre plusieurs décharges neuronales ("spike"). La distribution de ces intervalles est caractéristique de la dynamique neuronale. En fonction de plusieurs paramètres du processus de Wiener nous observons différentes classes de distributions ISI. Nous sommes particulièrment interessés par les distributions multimodales, qui peuvent être rapprochées à des observations expérimentales ou neurophysiologiques. Du point de vue du modèle nous analysons les conséquences des sauts dont la distribution des ISI suit une distribution exponentielle ou une distribution gaussienne inverse.

Contents

In this Chapter we illustrate the results obtained on the study of model (2.1.16) that are published in the papers [**53**], [**52**] and [**59**]. As mentioned in Chapter 2, this model have strong weaknesses from a biological point of view. Its analysis has been for us a preliminary study on jump diffusion models and a starting point to analyze then model (2.1.14) whose results are showed in Chapter 5. Indeed model (2.1.16) can be considered as a simpler version of model (2.1.14) with no exponential decay, i.e. the term governed by parameter θ, so that it is a model in which trajectories evolve in time with a linear growth perturbed by the stochastic term W, i.e. the Brownian motion.

We adopted an approach to jump diffusion models that is mainly based on the analysis of multimodal inter-spike intervals (ISIs). That is we observed that there exist ranges of the involved parameters that give rise to ISIs histograms with more than one single peak. As deeply explained in Chapter 5.2, this feature caught our attention. From a mathematical and phenomenological point of view it is kind of unexpected property of the random variable FET (2.1.2). Indeed the first passage time of a Wiener process (the diffusive part of model (2.1.16)) through a constant threshold S has unimodal probability density function (4.1.2) and the FET of a pure jump process $J = \{J_t, t \geq 0\}$ obtained as

$$J_t = a_+ N_t^+ + a_- N_t^-, \tag{4.0.5}$$

where $J_0 = 0$ and a_+, a_-, N^+ and N^- are the same as in eq. (2.1.16), i.e. the discrete part of the model, shows, for the chosen range of the parameters, unimodal histograms on a very large time scale. Moreover, histograms with more than one single peak, remind p.d.f.

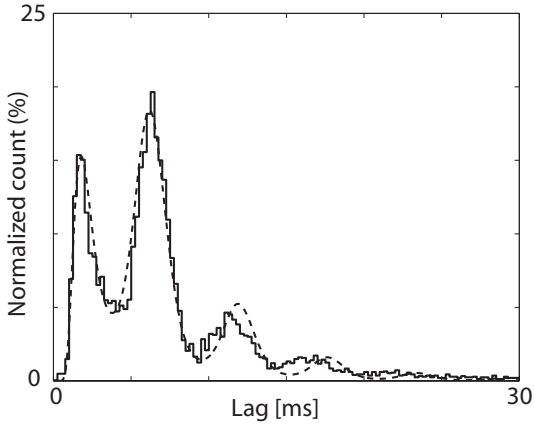

FIGURE 4.1. ISIs distributions from models (2.1.16) and (4.0.6). In model (2.1.16) $\mu = 1.5$ mVms^{-1}, $\sigma^2 = 0.25$ mV^{2}ms^{-1}, $a_+ = -a_- = 7.5$ mV and $\lambda^+ = \lambda^- = 100$ ev/s, $S = 10$ mV, $V_{rest} = 0$ mV (continuous line) and in model (4.0.6) $\tilde{\mu} = 1.5$ mVms^{-1}, $\tilde{\sigma}^2 = 8.25$ mV^{2}ms^{-1}, $\tilde{S} = 11$ mV, $\tilde{V}_{rest} = 0$ mV, $q = -2.42$, $\nu = 1.1$ and $\phi = 2.7708$ (dashed line).

obtained for the first passage time of diffusive models with forcing oscillatory drift term (cf. [**10**], [**11**], [**35**], [**39**], [**57**] and references quoted therein). In particular we showed that there exists a range in the parameters space of model (2.1.16) that allow to completely reproduce (cf. Fig. 4.1) the p.d.f. obtained for the first passage time of the process $V^{OB} = \{V_t^{OB}, t \geq 0\}$

considered in [**10**] and given by

$$\begin{aligned} dV_t^{OB} &= [\tilde{\mu} + q\cos(\nu t + \phi)]\, dt + \tilde{\sigma} dW_t \\ V_0^{OB} &= \tilde{V}_{rest}. \end{aligned} \tag{4.0.6}$$

where W is a Wiener process and an external periodic force of frequency $\nu > 0$, intensity $q > 0$ and phase ϕ is applied. This fact let arise many questions like which are similarities and differences between jump-diffusion models and models with oscillatory drift.

From a bio-modelling point of view as well, multi-peak ISIs histograms are particularly interesting. But we postpone a detailed discussion about that subject in Chapter 5.2 where we discuss the results obtained for model (2.1.14). Indeed we analyze model (2.1.16) only from a phenomenological point of view since we believe that it is an excessive simplification of the neurophysiological properties of a neuron and it makes inadequate a reinterpretation of the results in a biological framework.

4.1. Results

We will not pay attention, in this preliminary study, to the physiological agreement of the parameters values, target that we are going to deal with very carefully when studying model (2.1.14). Our goal is to illustrate features of the model related with the coupling of the two random sources (the diffusion process and the jump processes) and arising with the introduction of the non linearity, i.e. the threshold. We consider only the process V^{WJ} reset to its resting value after each spike, i.e. the case that we called *closed circuit* (cf. Fig. 2.4*a*). If not differently stated, we choose $\lambda^+ = \lambda^-$ and $a_+ = a_-$, i.e. the jump processes affect the dynamics with null total contribution. We fix $S = 10$ mV and $V_{rest} = 0$ mV. We divide in two Sections the analysis. In Section 4.1.1 we consider jump processes N^+ and N^- that are two independent homogeneous Poisson processes. In Section 4.1.2 we consider jump processes with inter-event IG distributed.

4.1.1. Jump processes with Exponentially distributed inter-arrival times. We consider here that N^+ and N^- in eq. (2.1.16) are two independent homogeneous in time Poisson processes with $N_0^+ = N_0^- = 0$ and intensities λ^+ and λ^- respectively. Here follows a summary of the results.

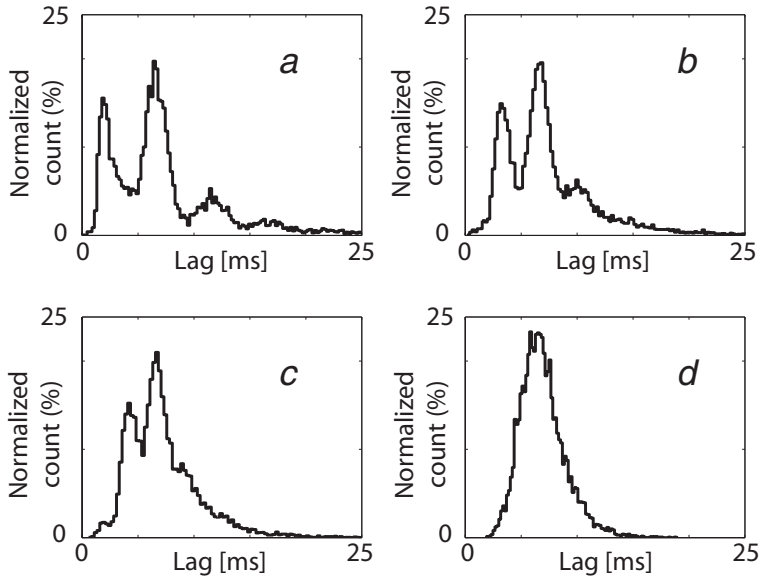

FIGURE 4.2. Simulated ISI distribution of the model (2.1.16) with Poisson jump processes as jump amplitudes $a_+ = -a_-$ [mV] vary. Here $\mu = 1.5$ mVms^{-1} and $\sigma^2 = 0.25$ mV^{2}ms^{-1}, $\lambda^+ = \lambda^- = 10$ ev/s, $a_+ = 7.5$ (**a**), $a_+ = 5.5$ (**b**), $a_+ = 4$ (**c**) and $a_+ = 2.5$ mV (**d**)

As the jumps amplitudes $a_+ = a_-$ decrease, ISIs histograms become unimodal (cf. Fig. 4.2). It means that to detect multimodal histograms the jumps amplitudes need to be sufficiently big with respect to the threshold level. Thus in accordance with the diffusive limit theorems that suppose jumps amplitudes going to zero (cf. eq. (2.1.5) and [**25**]). In Fig. 4.3 the ISIs histograms for different values of the jump processes intensities $\lambda^+ = \lambda^-$ are plotted. It appears that as $\lambda^+ = \lambda^-$ increase the peaks at larger lags disappear and the probabilistic mass accumulates at shorter lags making the first peak the highest one. It is possible to notice as well a strong regularity in the position of the peaks as $\lambda^+ = \lambda^-$ vary. We may make the hypothesis that the lag of each peak is given by the mode of the first passage time of a Wiener process without jumps (2.1.6) through different constant thresholds

$$S - a_+,\ S,\ S + a_+,\ S + 2a_+, ... = S + ka_+, \text{ where } k = -1, 0, 1, 2, ... \tag{4.1.1}$$

Named $m(S)$ the mode of an IG$(|S|/\mu, S^2/\sigma^2)$ distribution with threshold S, given by the following expression

$$m(S) = \sqrt{\frac{S^2}{\mu^2} + \frac{9\sigma^4}{4\mu^4}} - \frac{3\sigma^2}{2\mu^2}, \tag{4.1.2}$$

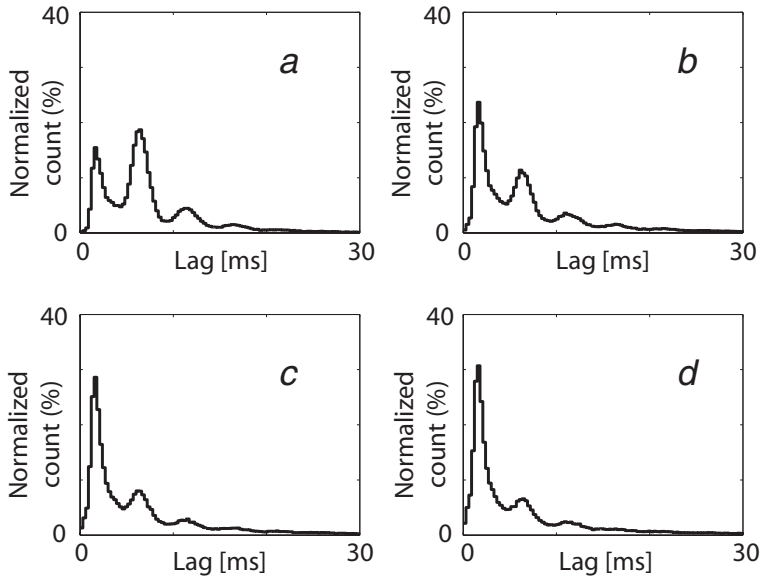

FIGURE 4.3. Simulated ISI distribution of the model (2.1.16) with Poisson jump processes as $\lambda^+ = \lambda^-$ [ev/s] increase. Here $\mu = 1.5$ mVms^{-1}, $a_+ = a_- = 7.5$ mV, $\sigma^2 = 0.25$ mV^{2}ms^{-1}, $\lambda^+ = \lambda^- = 100$ in (**a**), $\lambda^+ = \lambda^- = 200$ in (**b**), $\lambda^+ = \lambda^- = 300$ in (**c**) and $\lambda^+ = \lambda^- = 400$ ev/s in (**d**).

the peaks lags will be $m(S + ka_+)$, with $k = -1, 0, 1, 2, ...$ This fact is confirmed in Fig. 4.4. As the drift parameter of the diffusive part of the model increases, the peaks lags shorten following eq. (4.1.2), the FET becomes faster and the tail slims. Increasing the diffusive coefficient (second order infinitesimal moment) σ^2 the FETs spread out on the time axis giving rise to heavier tails and less marked multimodality (cf. Fig. 4.5). In Fig. 4.6 the model is considered when receiving only inhibitory strong inputs and no excitatory ones, i.e. with $a_+ = 0$ mV. There, multimodal ISIs histograms show longer tails with regular peaks as the intensity of the jump process N^- increases.

4.1.2. Jump processes with Inverse Gaussian distributed inter-arrival times. We consider here that N^+ and N^- in eq. (2.1.16) are two independent point processes with $N_0^+ = N_0^- = 0$ and inter-events distributed according to IG$(|S_+|/\mu_+, (S_+)^2/\sigma_+^2)$ and IG$(|S_-|/\mu_+, S_-^2/\sigma_-^2)$ respectively. We fix $S^+ = S^- = 10$ mV. Here follows a summary of the results.

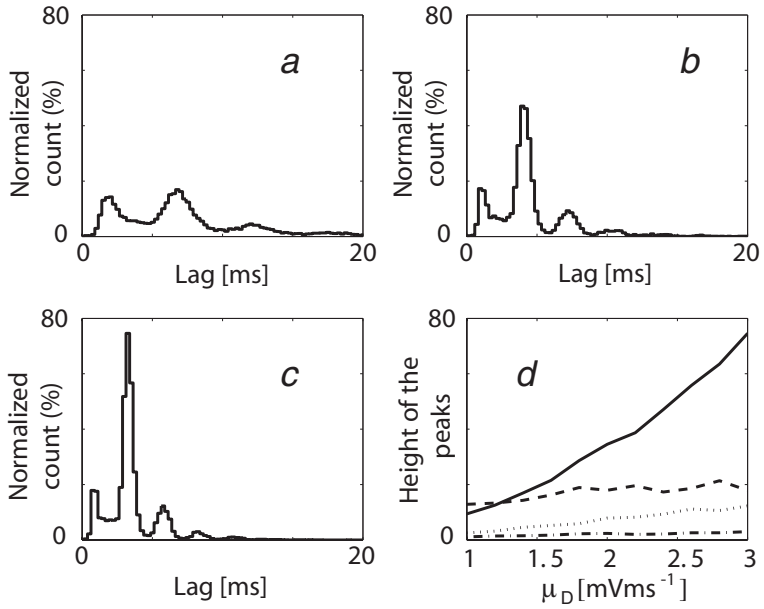

FIGURE 4.4. Simulated ISI distribution of the model (2.1.16) with Poisson jump processes as μ [mVms^{-1}] varies. Here $\sigma^2 = 0.25$ mV^{2}ms^{-1}, $\lambda^+ = \lambda^- = 100$ ev/s, and $a_+ = -a_- = 7.5$ mV, $\mu = 1.4$ (**a**), $\mu = 2.4$ (**b**) and $\mu = 3.0$ mVms^{-1} (**c**). In (**d**) the height of the first four peak versus μ is plotted. From the first to the fourth peak the lines are dotted, continuous, dashed and dash-dotted respectively.

As the drift parameters $\mu_+ = \mu_-$ in the IG distribution governing the inter-events distribution of the jump processes, i.e. the frequency of occurrences, decrease (cf. Fig. 4.7) ISIs histograms become unimodal. It is noticeable that the peaks lags are affected by changes in $\mu_+ = \mu_-$ values. The peaks position seems determined by the jump processes and in particular by multiples of the mode m of the inter-events distributions given by (4.1.2) so that the k-th peaks lies at lag $k \cdot \mu$, with $k \in \mathbb{N}$. As the inter-times between successive jumps increase their variances $\sigma_+^2 = \sigma_-^2$, multimodality disappears (cf. Fig. 4.8). On the other hand as the diffusion coefficient σ^2 of the underlying diffusion process increases (cf. Fig. 4.9) the tail lengthen and let appear regularly more peaks in the histograms. In Fig. 4.10 the model is considered when receiving only inhibitory strong inputs and no excitatory ones, i.e. with $a_+ = 0$ mV. It is shown that increasing the frequency of the jumps, the histograms becomes sharply multimodal.

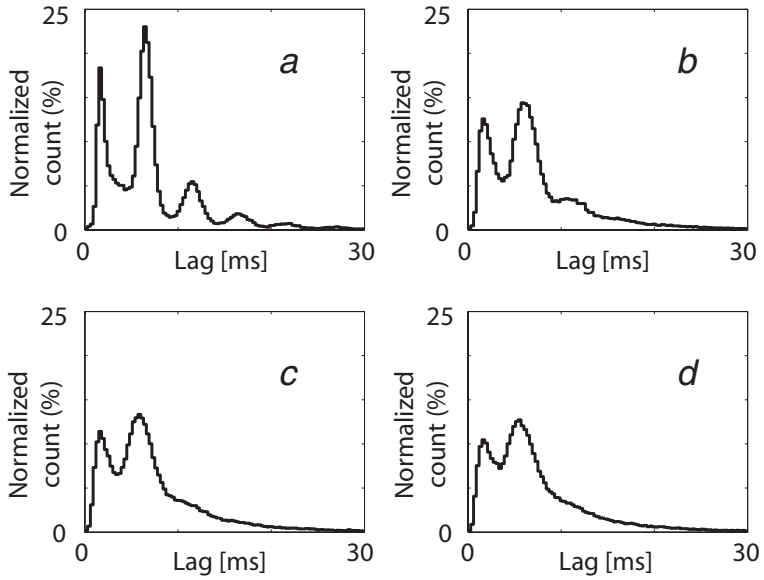

FIGURE 4.5. Simulated ISI distribution of the model (2.1.16) with Poisson jump processes as σ^2 [mV^{2}ms^{-1}] increases. Here $\mu = 1.5$ mVms^{-1}, $\lambda^+ = \lambda^- = 100$ ev/s, $a_+ = a_- = 7.5$ mV, $\sigma^2 = 0.15$ mV^{2}ms^{-1} in (**a**), $\sigma^2 = 0.5$ mV^{2}ms^{-1} in (**b**), $\sigma^2 = 0.75$ mV^{2}ms^{-1} in (**c**) and $\sigma^2 = 1$ mV^{2}ms^{-1} in (**d**).

4.2. Discussion

From the preliminary study of the jump-diffusion model made up by the superimposition of a Wiener process with drift and two counting processes (2.1.16) it is possible to conclude, in the first resort, that the dynamics of the membrane potential are very different whether the inter-times between successive jumps are Exponentially distributed or IG distributed. The peaks lags are determined by the diffusion parameters when the jump processes are Poisson processes (cf. Fig. 4.4), while they results determined by the jumps parameters when IG inter-distributed (cf. Fig. 4.7). These results seem due to the fact that, if IG inter-distributed, the jump processes dominate the dynamics establishing the time lags of the crossing of the threshold. This fact is confirmed as well by the different behavior of the two models with respect to changes in the value of the diffusive parameter σ^2. When the jumps are Poisson processes an increase in the value of σ^2 hides the peaks in the ISIs histograms in particular in the tails that become heavier (cf. Fig. 4.5). But when the jumps are IG inter-distributed (cf. Fig. 4.9), increasing the diffusive coefficient makes the ISIs

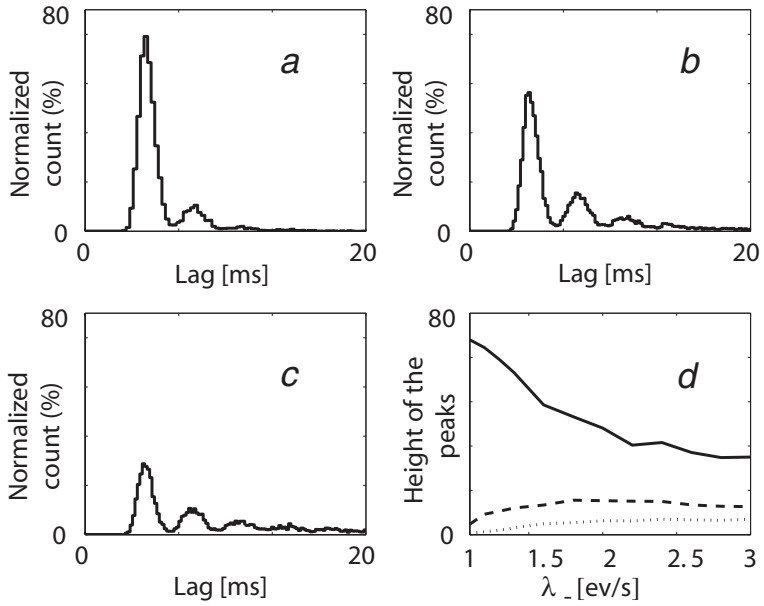

FIGURE 4.6. Simulated ISI distribution of the model (2.1.16) with Poisson jump processes as jump intensity λ^- [ev/s] vary and with $a_+ = 0$ mV. Here $\mu = 1.5$ mVms^{-1}, $\sigma^2 = 0.25$ mV^{2}ms^{-1}, $a_+ = 0$ mV and $a_- = -7.5$ mV, $\lambda^- = 20$ (**a**), $\lambda^- = 80$ (**b**) and $\lambda^- = 180$ ev/s (**c**). In (**d**) the heights of the first three peak height versus λ^- is plotted. From the first to the third peak the lines are continuous, dotted and dashed respectively.

more clearly multimodal and the tails let emerge new peaks. The dynamics in this case is dominated by the jump processes that produce events (EPSP or IPSP) at very regular time intervals and better emerge from a more scattered underlying diffusion process. The way the two random sources (the jump processes and the diffusion process) couple together is very different according to the distribution of the jump processes. This remark will be confirmed as well when the underlying diffusion process will be an Ornstein Uhlenbeck process (2.1.14).

This first study gives an idea about the influence of each parameter on the model. But it is restricted to a phenomenological approach. We would like to recall that the range of the parameters values that let appear multimodal ISIs histograms is quite small. Moreover it further narrows when considering the jump-diffusion model with OU underlying diffusion process (2.1.14). So this analysis allowed to acquire the knowledge necessary to face the study of a more complex model such as (2.1.14).

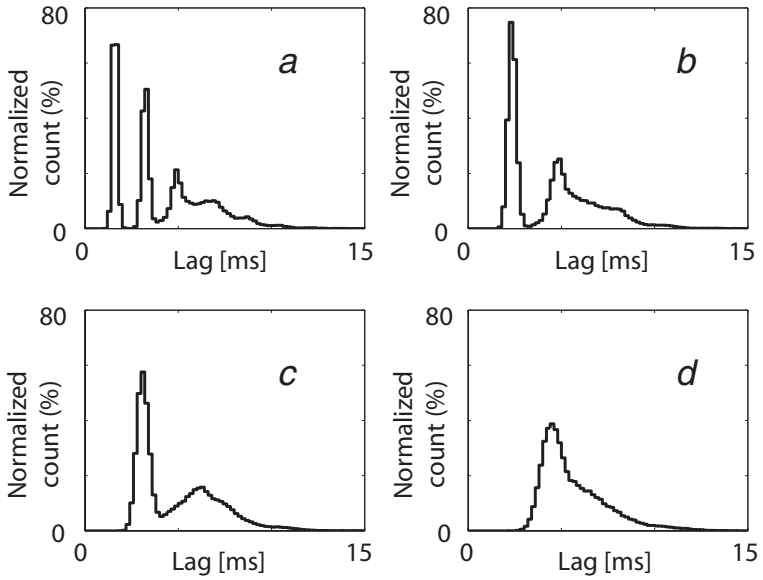

FIGURE 4.7. Simulated ISI distribution of the model (2.1.16) with IG jump processes as $\mu_+ = \mu_-$ [mVms^{-1}] decrease. Here $\mu = 1.5$ mVms^{-1}, $\sigma^2 = 1$ mV^{2}ms^{-1}, $\sigma_+^2 = \sigma_-^2 = 0.5$ mV^{2}ms^{-1} and $S^+ = S^- = 10$ mV, $\mu_+ = \mu_- = 6$ mVms^{-1} in (**a**), $\mu_+ = \mu_- = 4$ mVms^{-1} in (**b**), $\mu_+ = \mu_- = 3$ mVms^{-1} in (**c**) and $\mu_+ = \mu_- = 2$ mVms^{-1} in (**d**).

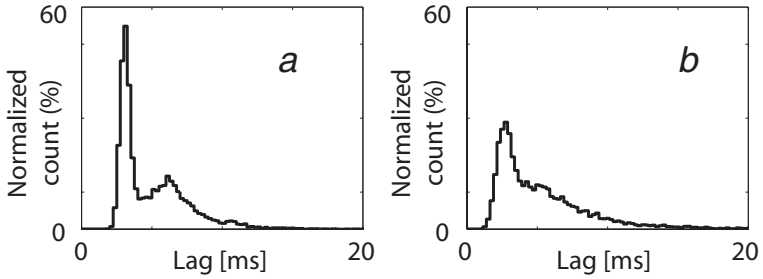

FIGURE 4.8. Simulated ISI distribution of the model (2.1.16) with IG jump processes as $\sigma_+ = \sigma_-$ [mV^{2}ms^{-1}] vary. Here $\mu = 1.5$ mVms^{-1} and $\sigma^2 = 2$ mV^{2}ms^{-1}, $\mu_+ = \mu_- = 3$ mVms^{-1}, ${\sigma_+}^2 = 3$ (**a**) and ${\sigma_+}^2 = 0.5$ mV^{2}ms^{-1} (**b**).

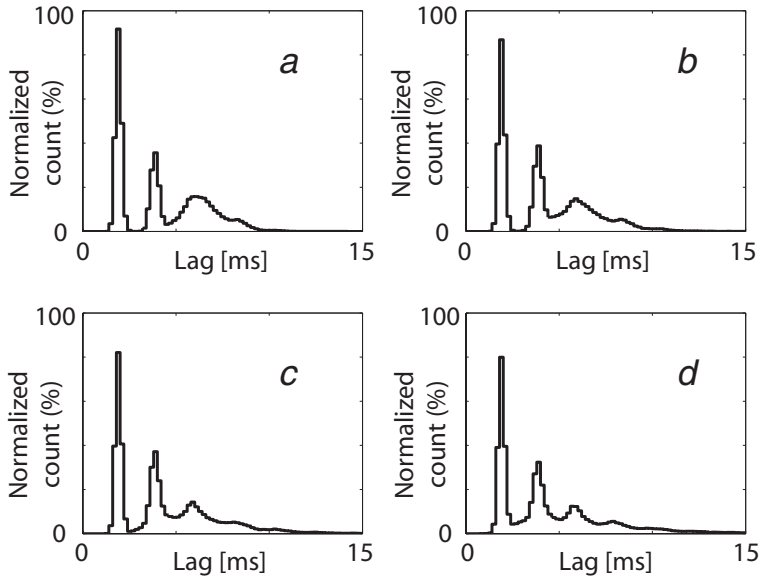

FIGURE 4.9. Simulated ISI distribution of the model (2.1.16) with IG jump processes as σ^2 [mV^{2}ms^{-1}] increases. Here $\mu_+ = \mu_- = 5$ mVms^{-1}, $\sigma_+^2 = \sigma_-^2 = 0.5$ mV^{2}ms^{-1}, $\mu = 1.5$ mVms^{-1}, $\sigma^2 = 0.5$ in (**a**), $\sigma^2 = 1$ in (**b**), $\sigma^2 = 2$ in (**c**) and $\sigma^2 = 4$ mV^{2}ms^{-1} in (**d**).

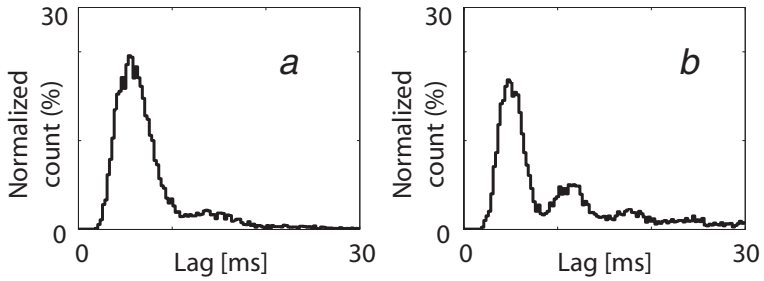

FIGURE 4.10. Simulated ISI distribution of the model (2.1.16) with IG jump processes as μ_- [mV] varies and $a_+ = 0$ mV. Here $\mu = 1.5$ mVms^{-1}, $\sigma^2 = 2$ mV^{2}ms^{-1} and $\sigma_-^2 = 0.5$ mV^{2}ms^{-1}, $\mu_- = 1$ (**a**) and $\mu_- = 1.5$ mVms^{-1} (**b**).

CHAPTER 5

An Ornstein Uhlenbeck process with jumps as a neuronal model

Résumé Le chapitre 5 étudie le modèle de saut-diffusion dans lequel la diffusion est donnée par un processus d'Ornstein Uhlenbeck. De manière similaire au chapitre precédent nous analysons ici les effets des processus de sauts dont la distribution temporelle suit une distribution exponentielle ou une distribution gaussienne inverse. Dans les deux cas nous observons des distributions multimodales. Dans une marge restreinte de l'espace des paramètres nous observons la présence d'un phénomène nouveau, décrit ici pour la première fois. Il s'agit d'un phénomène de type résonnant ("resonant like") dû à la composition du processus diffusif et des processus de saut correspondant aux afférences excitatrices et afférences inhibitrices. Cette observation suggère que pour certaines intensités des processus de saut afférents ("bruit de fond") un neurone peut participer à plusieures assemblées de cellules ("cell assemblies").

Contents

In the present Chapter we investigate multimodal ISI distributions in the case of a neuronal model corresponding to an Ornstein Uhlenbeck process with the superimposition of two jump processes with inter spikes intervals Exponentially and Inverse Gaussian distributed. The results here illustrated are collected in the paper [**60**]. The model describes the membrane

potential evolving in time following the jump diffusion process. The spike train corresponds to the sequence of times when the jump diffusion process crosses a constant threshold S. We analyze such model in two instances. In the first case the jump diffusion process is reset to its initial value any time the membrane potential crosses the threshold. The sequence of firing times is a renewal process and this case may be viewed as the activity of a small network with internal feedback, referred to as *closed circuit*. In the second case the jump processes are not reset to their initial value after the membrane potential crosses the threshold. In this case the generated spike train is not a renewal process and its dynamics may be the result of a small network without internal feedback, referred to as *open circuit*. These two versions of the model are introduced and discussed in detail in Section 2.1.2. In Section 5.1 we perform a systematic study of the parameters of the model that generate ISI histograms with more than one peak and we show the existence of optimal values of the noise intensity that can enhance the signal transmission. Finally in Section 5.2 we discuss our results in details both from a mathematical and a biological point of view.

5.1. Results

The main objective of this study is to determine the roles of the parameters that are involved in the neuronal model given by the jump-diffusion process defined by equation (2.1.14). The ranges of the parameters were selected near biological ranges but the values were not selected with the intention to test a specific physiologically valued model, but rather with the goal to study the qualitative features of the neuromimetic model. In particular we present results associated with the conditions that let appear a multimodal distribution of the inter-spike intervals. The peaks of the histogram may be considered as characteristic times of the neuron and may suggest multiple functional roles of the neuron, as discussed in Section 5.2.

Since no closed form expression is available for the density of the random variable T (2.1.2), this study is performed by means of simulations of the SDE (2.1.14). The simulation algorithm is presented in detail in Chapter 3.

5.1.1. Tuning of the parameters. Throughout this Chapter the resting potential is fixed to $V_{rest} = 0$ mV and the threshold to $S = 10$ mV, that corresponds to a simple

translation of physiological data values useful to simplify the mathematical analysis of the model. To represent the intensity of the strong inputs, large values of $a_+ = -a_- = 5$ mV are chosen with respect to the threshold value. Moreover, we study the model in a particular condition with balanced excitatory and inhibitory strong inputs, such that $a_+ = -a_-$ and, if not differently stated, the same probability of occurrence for the excitatory and inhibitory jumps are selected. Hence the sum of the jump processes results characterized by zero mean and avoids to mask the trend given by the diffusive part of the model.

The examples proposed in the next Subsections are consistent with the parameters of the common underlying diffusion process (2.1.11). The value of the time constant is kept fixed at $\theta = 10$ ms and the value of the diffusion coefficient at $\sigma^2 = 0.05$ mV^{2}ms^{-1}. The value of the drift μ of the Ornstein Uhlenbeck process (2.1.11) is $\mu = 0.7$ mVms^{-1} if the jump processes have inter-events Inverse Gaussian distributed and $\mu = 0.98$ mVms^{-1} if the jump processes are Poisson processes. This choice is determined by the fact that the range of the parameters values of the model that produce ISI distributions depends on the type of distribution of the jump processes. In both cases we choose the values of the parameters such that $\mu \cdot \theta < S$. Indeed for such range of the parameters values the dynamics of the Ornstein Uhlenbeck process is as much as possible different from the dynamics of the Wiener process we already studied in Chapter 4.

Simulation batches are performed with samples of $N = 10,000$ runs. At each run the spike trains (i.e., the epochs of the events) are recorded and the ISIs are calculated. The model is usually described by the ISI distributions and in some cases of interest the auto- and cross-correlation histograms are calculated according to [**1**], [**43**], [**44**] and [**2**] using the program available at *http://openAdap.net/*.

5.1.2. Jump processes with Inverse Gaussian distributed inter-arrival times. In this subsection we analyze the case of Inverse Gaussian (IG) distributed inter-event intervals in the jump processes. This means that the counting processes N_t^+ and N_t^- are generated with inter-event intervals distributed according to independent IG, eq. (2.1.7), with parameters $(|S_+|/\mu_+, S_+^2/\sigma_+^2)$ and $(|S_-|/\mu_-, S_-^2/\sigma_-^2)$ respectively.

The parameters that determine the dynamics of the process V_t described in eq. (2.1.15) can be naturally divided into two groups: the first group collects together the parameters

that drive the jump processes, while the second group gather the parameters that run the diffusion process.

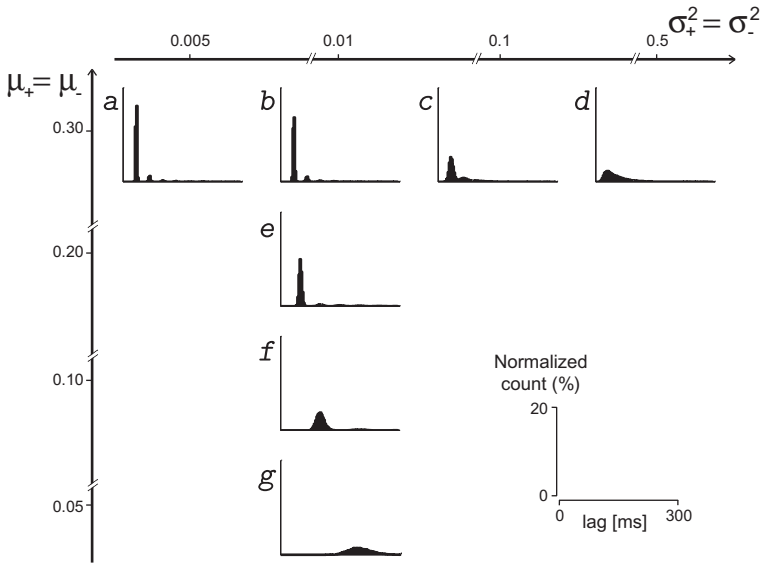

FIGURE 5.1. Dependency on parameters of the jump processes, $\mu_+ = \mu_-$ [mVms^{-1}] and on $\sigma_+ = \sigma_-$ [mV^{2}ms^{-1}]. *Open circuit* instance. Distributions of the first exit time of the process (2.1.14) with Inverse Gaussian distributed interarrival jumps through the constant threshold S. This corresponds to the ISI histograms of spike train A given an IG distribution of the input jumps processes of units E and I. Here $S = 10$ mV, $\mu = 0.7$ mVms^{-1}, $\theta = 10$ ms, $\sigma^2 = 0.05$ mV^{2}ms^{-1}, $S_+ = S_- = 10$ mV, and $a_+ = -a_- = 5$ mV. In (**a**, **b**, **c**, **d**) $\mu_+ = \mu_- = 0.3$ mVms^{-1}. In (**b**, **e**, **f**, **g**) $\sigma_+^2 = \sigma_-^2 = 0.01$ mV^{2}ms^{-1}. In (**a**) $\sigma_+^2 = \sigma_-^2 = 0.005$, (**b**) $\sigma_+^2 = \sigma_-^2 = 0.01$, (**c**) $\sigma_+^2 = \sigma_-^2 = 0.1$ and (**d**) $\sigma_+^2 = \sigma_-^2 = 0.5$. In (**b**) $\mu_+ = \mu_- = 0.3$, (**e**) $\mu_+ = \mu_- = 0.2$, (**f**) $\mu_+ = \mu_- = 0.1$ and (**g**) $\mu_+ = \mu_- = 0.05$.

5.1.2.1. *Dependency on the jump processes.* The parameters characterizing the diffusion process (2.1.11) are kept constant at values $\theta = 10$ ms, $\mu = 0.7$ mVms^{-1} and $\sigma^2 = 0.05$ mV^{2}ms^{-1}. The value $S_+ = S_- = 10$ mV is kept constant as well, but the parameters $\mu_+ = \mu_-$ and $\sigma_+^2 = \sigma_-^2$, are varied, i.e. the frequency and the variability of the jump processes are varied. Fig. 5.1 shows the ISI histograms in the *open circuit* instance (cf. Fig. 2.4*a*). It is interesting to notice that for small values of variance of the jumping times, i.e. the coefficients $\sigma_+^2 = \sigma_-^2$, it is possible to observe up to seven separate peaks in the ISI histograms (Fig. 5.1*a*). Conversely, larger values of variance of the jumping times provoke a loss of multimodality in the ISI histograms (Fig. 5.1*d*). The inter-times between successive jumps become longer and the ISI histograms show fewer peaks with small values of the

parameters $\mu_+ = \mu_-$ (Fig. 5.1*f,g*). The abscissae of the peaks is completely determined by the jump processes parameters. Named m the mode of the IG distribution given by the following expression

$$m = \sqrt{\frac{S_+^2}{\mu_+^2} + \frac{9\sigma_+^4}{4\mu_+^4}} - \frac{3\sigma_+^2}{2\mu_+^2}, \tag{5.1.1}$$

the peaks will appear at abscissae $t_m = km$, with $k \in \mathbb{N}$. The analysis of cross correlation histograms between the time series of firing times from units A, E and I represented in Fig. 5.1 show that the efficiency of both excitatory and inhibitory inputs is not affected by varying $\sigma_+^2 = \sigma_-^2$ and $\mu_+ = \mu_-$. It is worth reporting that in the case of the *close circuit* the results are very similar with respect to the changes in the shape of the ISI histograms at varying the parameters.

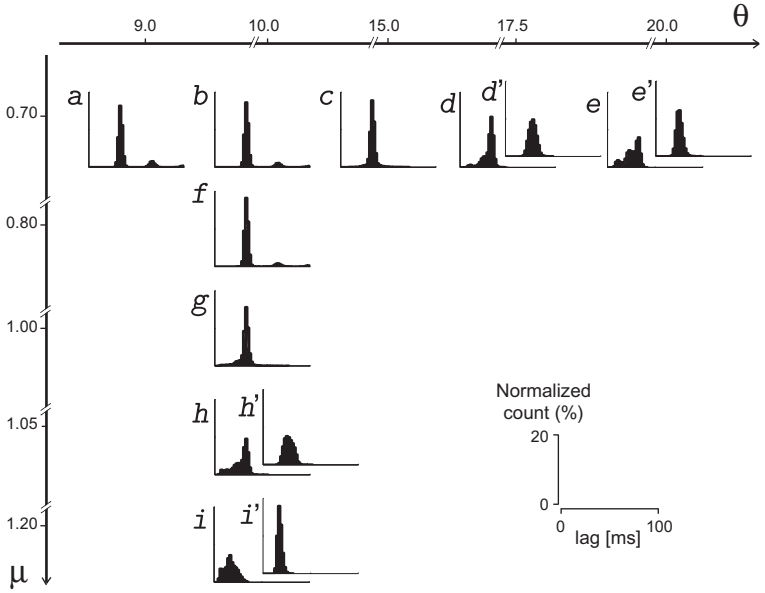

FIGURE 5.2. Dependency on parameters of the diffusion process, θ [ms] and on μ [mVms^{-1}]. Distributions of the first exit time of the process (2.1.14) with Inverse Gaussian distributed interarrival jumps through the constant threshold S. This corresponds to the ISI histograms of spike train A given an IG distribution of the input jumps processes of units E and I. Panels (**a**–**i**) refer to the *open circuit* instance. Panels (**d′**,**e′**,**h′**,**i′**) refer to the *closed circuit* instance. Here $S = 10$ mV, $\sigma^2 = 0.05$ mV^{2}ms^{-1}, $S_+ = S_- = 10$ mV, $\mu_+ = \mu_- = 0.3$ mVms^{-1}, $\sigma_+^2 = \sigma_-^2 = 0.01$ mV^{2}ms^{-1} and $a_+ = -a_- = 5$ mV. In (**a**, **b**, **c**, **d**, **d′**, **e**, **e′**) $\mu = 0.7$ mVms^{-1}. In (**b**, **f**, **g**, **h**, **h′**, **i**, **i′**) $\theta = 10$ ms. In (**a**) $\theta = 9$, (**c**) $\theta = 15$, (**d**, **d′**) $\theta = 17.5$ and (**e**, **e′**) $\theta = 20$ ms. In (**f**) $\mu = 0.8$, (**g**) $\mu = 1$, (**h**, **h′**) $\mu = 1.05$ and (**i**, **i′**) $\mu = 1.2$ mVms^{-1}.

5.1.2.2. *Dependency on the diffusion process.* The parameters that drive the counting processes N_t^+ and N_t^- are kept constant to the values $S_+ = S_- = 10$ mV, $\mu_+ = \mu_- = 0.3$ mVms^{-1} and $\sigma_+^2 = \sigma_-^2 = 0.01$mV^{2}ms^{-1}. Fig. 5.2 shows the ISI histograms of cell N as a function of the coefficients μ and θ in the diffusion process, eq. (2.1.11). With combination of parameter ranges such that $\theta \leq 15$ and $\mu \leq 1$ (Fig. 5.2*a,b,c,f,g*) the results obtained with both *open* and *closed circuits* are very similar and show a multimodal distribution characterized by the first peak as the highest one. In the non renewal model (*open circuit*) the ISI histograms are also multimodal for larger values of θ and μ but the shape is very different and the last peak is the highest one (Fig. 5.2*d,e,h,i*). On the opposite, the diffusive part of the jump diffusion process, i.e. the Ornstein Uhlenbeck process, is the dominating process for larger values of θ and μ in the renewal case (*closed circuit*). In this case Fig. 5.2*d′, e′,h′,i′* show FETs with an estimated p.d.f. that can be overlapped to the p.d.f. of the first passage time of only an Ornstein Uhlenbeck process through a constant boundary. This suggests the existence of two different dynamics of the model associated to the two domains in the space of the parameters θ and μ. In the *open circuit* case the spike trains of the reference unit A, of the excitatory input E and of the inhibitory input I have been analyzed in detail in the time domain by means of the auto- and cross-correlation histograms. Fig. 5.3*a* shows the analysis for the pair of units (A, E) with parameters $\theta = 17.5$ and $\mu = 0.7$. All correlograms show many oscillations due to the pacemaker-like activity of cells E and I when inter-spikes intervals are IG distributed. The asymmetrical peak on the left side of time zero, at lags $1 - 2$ms, denotes the high probability that unit E fires just before unit A. Fig. 5.3*b* shows the analysis for the pair of units (A, I) given the same previous set of parameters θ and μ. It is interesting to notice that the autocorrelograms of units E and I are very similar but their different timings produce a totally different cross-correlogram. The asymmetrical trough on the left side of time zero in the cross-correlogram of pair (A, I) denotes the low probability that unit E fires at short lags before unit A. In Fig. 5.3*c* we examine the area of the nearest peak or trough to time zero beyond the 99% limits of confidence of the correlogram as θ varies. This area is expressed in "events" units. In the case of pair (A, E) the peak area corresponds to the fraction of E events that contribute to the firing of unit A, which may be interpreted as the "excitatory efficiency" of the E input. In the case of pair (A, I) the trough area may be interpreted as the "inhibitory efficiency" of the I input. Two domains of these curves are ideally separated in the parameter space by the critical value $\bar{\theta} = 14.28$

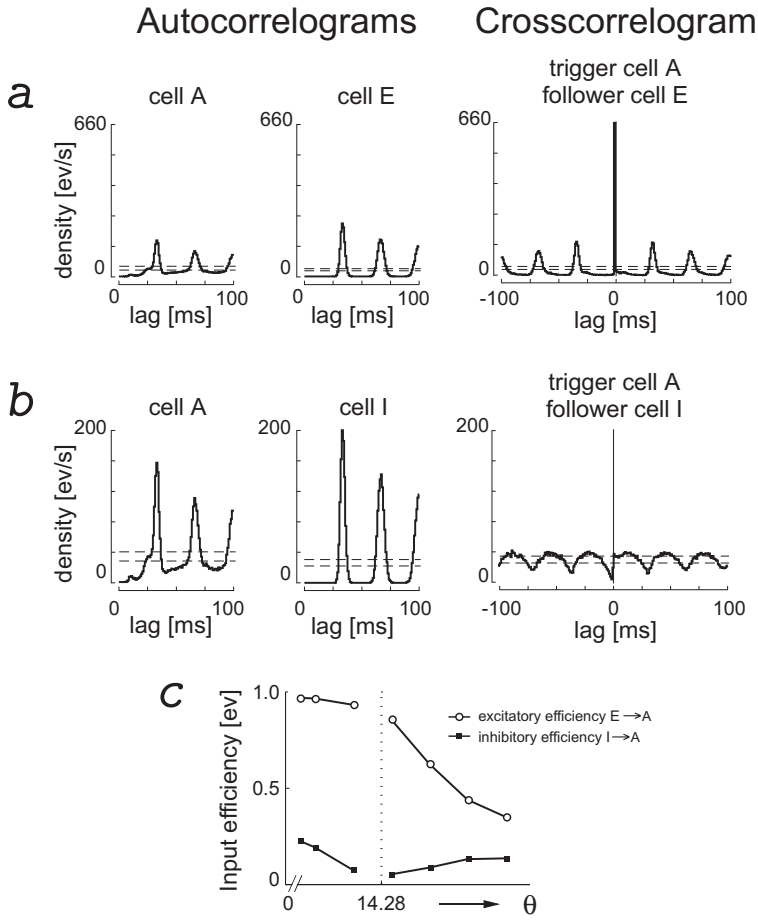

FIGURE 5.3. Dependency on parameter θ [ms] of the diffusion process. Crosscorrelation analysis in the *open circuit* instance. (**a**) Correlation analysis for the pair of units (A, E) with 99% confidence limits (dashed lines) calculated according to [**1**]. Notice the asymmetrical narrow peak on the left side near time zero in the crosscorrelogram. Here $\theta = 17.5$ ms and $\mu = 0.7$ mVms^{-1}, i.e. the same as in Fig. 5.2*d*. The other parameters are $S = 10$ mV, $\sigma^2 = 0.05$ mV^{2}ms^{-1}, $S_+ = S_- = 10$ mV, $\mu_+ = \mu_- = 0.3$ mVms^{-1}, $\sigma_+^2 = \sigma_-^2 = 0.01$ mV^{2}ms^{-1} and $a_+ = -a_- = 5$ mV. (**b**) Correlation analysis for the pair of units (A, I) with the same parameters of the model as in panel (**a**). (**c**) Dependency of "excitatory" and 'inhibitory efficiency" (see text for definitions) on parameter θ. Notice the existence of a subthreshold and a suprathreshold regime for θ less than and greater than $\theta = 14.28$ ms, respectively.

(Fig. 5.3*c*). The "excitatory efficiency" is stable or slowly decreases as $\theta < \bar{\theta}$ increases but it decreases very steadily as $\theta > \bar{\theta}$. The "inhibitory efficiency" decreases as $\theta < \bar{\theta}$ increases but

it reaches a minimum at $\theta = \bar{\theta}$ and it increases for parameter values $\theta > \bar{\theta}$. The meaning of the critical value of $\bar{\theta}$ on the model dynamics can be easily interpreted. The value $\bar{\theta} = 14.28$ is calculated such that $\mu \cdot \theta = S$. In the range $\mu \cdot \theta < S$ the Ornstein Uhlenbeck process, eq. (2.1.11), crosses the constant boundary S exclusively due to the stochastic part of the process. Then, the range of parameters $\mu \cdot \theta < S$ determines a *subthreshold* regime. Conversely, in the range $\mu \cdot \theta > S$, the crossing is mainly due to the deterministic trend of the process, which charaterizes a *suprathreshold* regime.

5.1.2.3. *Resonant like behavior.* In the current model, eq. (2.1.15), a random input term (i.e., the two counting processes) is superimposed to the same underlying Ornstein Uhlenbeck process. The analysis of the resulting process can be performed as a function of the coupling of the two random sources. A similar approach has been performed in [**10**], [**11**], [**35**], [**39**], and [**57**]. In the quoted papers the term stochastic resonance refers to noise induced enhancement in the detection and transmission of a signal and it goes with a deterministic oscillatory input term in a stochastic model. The absence of a pure oscillatory term in model (2.1.15), and hence of a period, does not allow a fully analogous description with stochastic resonance and so we use the term "resonance like" to denote noise induced phenomena. Moreover the analysis is here restricted to the heights of the peaks of the ISI histograms as σ^2 (the noise intensity) varies, recalling that their positions is here determined by the mode m of the IG distribution, that is a possible analogous of the period of the oscillatory term of previously described models [**11**], [**57**]. In the case of the *closed circuit* (i.e., with reset of the input process) the second peak of the ISI histogram, at lag t_2, was the significant one for this analysis (Fig. 5.4*a-d*). Figure 5.4*e* shows that a level of noise corrresponding to $\sigma^2 = 0.5$ lets appear more firing patterns of unit A characterized by ISIs equal to lag t_2 than other investigated levels of noise. In the case of the *open circuit* (i.e., without any reset of the input process) it is the first peak of the ISI histograms that goes through a maximum as the noise intensity σ^2 increases (Fig. 5.4*f-l*). The efficiency of the excitatory and inhibitory inputs were calculated by the crosscorrelogram analysis, as indicated in the previous Subsection, but no dependence on the level of the input noise σ^2 could be observed.

5.1.3. Jump processes with Exponentially distributed inter-event times. In this Subsection we examine the model when the two counting processes N_t^+ and N_t^- are

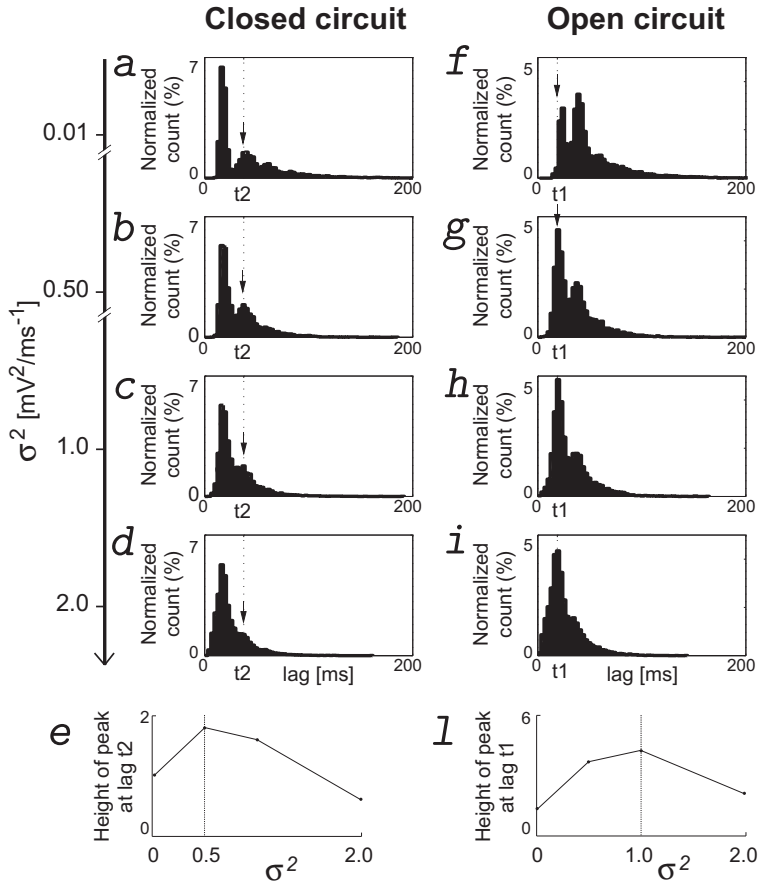

FIGURE 5.4. Dependency on σ^2 [$\mathrm{mV^2ms^{-1}}$]. Distributions of the first exit time of the process (2.1.14) with Inverse Gaussian distributed interarrival jumps through the constant threshold S. This corresponds to the ISI histograms of spike train A given an IG distribution of the input jumps processes of units E and I. Left panels correspond to the *closed circuit* and right panels to the *open circuit* instance. Here $S = 10$ mV, $\mu = 0.7$ $\mathrm{mVms^{-1}}$, $\theta = 10$ ms, $S_+ = S_- = 10$ mV, $\mu_+ = \mu_- = 0.05$ $\mathrm{mVms^{-1}}$, $\sigma_+^2 = \sigma_-^2 = 0.2$ $\mathrm{mV^2ms^{-1}}$ and $a_+ = -a_- = 5$ mV. (**a**,**f**) $\sigma^2 = 0.01$. (**b**, **g**) $\sigma^2 = 0.5$. (**c**, **h**) $\sigma^2 = 1$. (**d**, **e**) $\sigma^2 = 2$. (**e**) Resonant like behavior in the *closed circuit* instance. The height of the second peak (lag t_2) goes through a maximum for σ^2=0.5. (**f**) Resonant like behavior in the *open circuit* instance. The height of the first peak (lag t_1) goes through a maximum for σ^2=1.0.

Poisson processes, i.e. with intervals between events that are distributed according to Exponential distributions of parameters λ^+ and λ^- so that mean and variability of the process are given by $\mathbb{E}(N_t^+) = t\lambda^+ = Var(N_t^+)$. In this case the spike trains of units E and I are much more scattered and irregular in time than in the previous subsection where the inter-spike

intervals were IG distributed. The drift parameter of the diffusion process is fixed to the value $\mu = 0.98$ mVms^{-1} that determines a subthreshold regime where the crossing of the threshold S is caused only by the random part of the process (2.1.11).

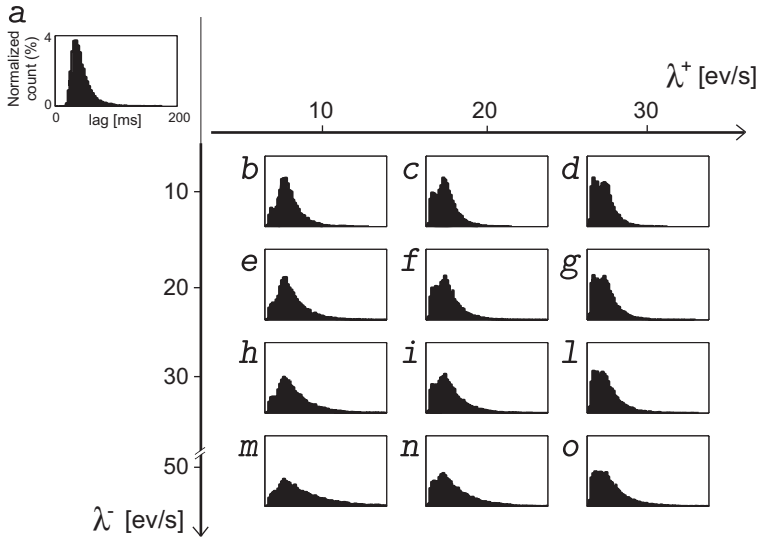

FIGURE 5.5. Dependency on the rate of the excitatory λ^+ [ev/s] and inhibitory inputs λ^- [ev/s]. Distributions of the first exit time of the process (2.1.14) with Exponentially distributed interarrival jumps through the constant threshold S. This corresponds to the ISI histograms of spike train A given a Poisson distribution of the input jumps processes of units E and I. Here $S = 10$ mV, $\mu = 0.98$ mVms^{-1}, $\theta = 10$ ms, $\sigma^2 = 0.05$ mV^{2}ms^{-1}. (**a**) Reference histogram with $a_+ = a_- = 0$ mV. In (**b**, **c**, **d**) $\lambda^- = 10$ ev/s; (**b**) $\lambda^+ = 10$; (**c**) $\lambda^+ = 20$; (**d**) $\lambda^+ = 30$. In (**e**, **f**, **g**) $\lambda^- = 20$ ev/s; (**e**) $\lambda^+ = 10$; (**f**) $\lambda^+ = 20$; (**g**) $\lambda^+ = 30$. In (**h**, **i**, **l**) $\lambda^- = 30$ ev/s; (**h**) $\lambda^+ = 10$; (**i**) $\lambda^+ = 20$; (**l**) $\lambda^+ = 30$. In (**m**, **n**, **o**) $\lambda^- = 50$ ev/s; (**m**) $\lambda^+ = 10$; (**n**) $\lambda^+ = 20$; (**o**) $\lambda^+ = 30$.

Figure 5.5 shows the histograms of the FETs following the variation of λ^+ and λ^-. Notice that the ISI histograms of the reference spike train A are identical in both *open* and *closed* circuit models if the jump processes N_t^+ and N_t^- are Poisson processes. This is due to the *memoryless* property of the Exponential distribution. The histograms of Fig. 5.5 show two peaks at most and a long tail, a very different shape with respect to the cases illustrated in Fig. 5.1 and Fig. 5.2. The first peak in Fig. 5.5 is driven by parameter λ^+ and is due to the probability mass of the trajectories that reach the threshold S following one upward jump. The lag of the first peak is not affected but its height is increased as λ^+ is increased, as illustrated in the series of panels of Fig. 5.5*b*-*d*, Fig. 5.5*e*-*g*, Fig. 5.5*h*-*l*, and Fig. 5.5*m*-*o*. The

second peak of the histograms is determined by the diffusion process and stays practically unchanged when λ^+ is increased. Indeed this peak is due to the FETs of trajectories that reach the boundary without jumps (upward or downward) or with an equal number of positive and negative jumps. The parameter λ^- affects the tail of the histogram, making it longer and heavier, such that the height of both peaks is slightly decreased as λ^- is increased but with no more peaks appearing. With parameters $\lambda^+ = 30$ ev/s and $\lambda^- = 10$ ev/s the auto- and cross-correlograms of the units pairs (A, E) and (A, I) are shown in Fig. 5.6*a* and Fig. 5.6*b*, respectively. The asymmetrical peak on the left side of the (A, E) crosscorrelogram indicates that there is a high probability that unit E is firing at short lags before unit A. Conversely, the trough on the left side of the (A, I) crosscorrelogram indicates that there is a low probability that unit I is firing at short lags before unit A.

The inhibitory effect of unit I on unit A is linear, as shown in Fig. 5.6*c* by the decrease in the firing rate of A as the firing rate of I (i.e., λ^-) is increased, independent of the rate λ^+. Figure 5.6*d* shows the "excitatory efficiency" (i.e., the peak area in the (A, E) crosscorrelograms) as a function of an increase in the rate of inhibition, λ^-. It is remarkable to notice a counterintuitive result. An increase in λ^- provokes a linear increase of the "excitatory efficiency" for any tested λ^+.

5.2. Discussion

We studied the firing pattern of an integrate and fire neuromimetic model whose membrane potential dynamics is described by a jump diffusion process, eq. (2.1.15). The spike train is obtained by the epochs of successive first exit times of the process from the strip $(-\infty, S]$. The main objective we pursued was to describe a range of the parameters of the model such that the inter-spike intervals (ISI) histograms are characterized by a multimodal distribution. In the absence of a pacemaker or of an oscillatory input the existence of such range of the parameters is of particular interest because the lag of each peak of the histogram is one of the times at which that neuron fires with higher probability (its "characteristic time"). The general hypothesis is that "global" parameters could affect the membrane excitability not of only one neuron but of an entire brain circuit such that more than one characteristic time could appear in the firing pattern under specific conditions not associated to a particular stimulus. In biology, the existence of the so-called non-specific pathways,

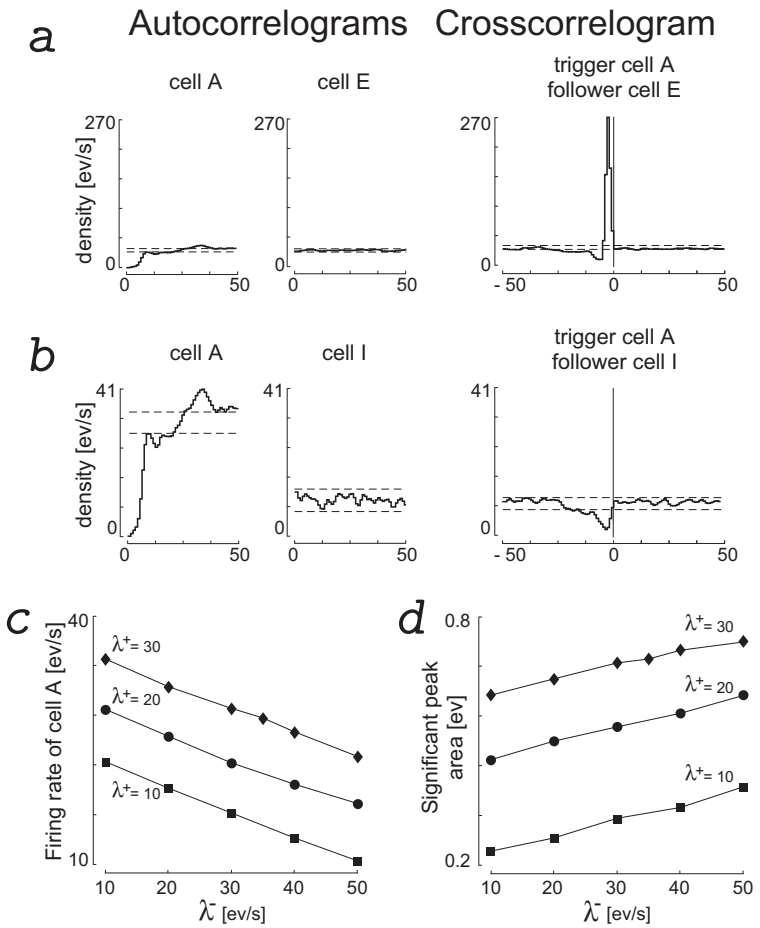

FIGURE 5.6. Dependency on the rate of the excitatory λ^+ [ev/s] and inhibitory inputs λ^- [ev/s] that follow a Poisson distribution. Here $S = 10$ mV, $\mu = 0.98$ mVms^{-1}, $\theta = 10$ ms, $\sigma^2 = 0.05$ mV^{2}ms^{-1}. (**a**) Correlation analysis for the pair of units (A, E) with 99% confidence limits (dashed lines) calculated according to [**1**]. The parameters of the jump processes are $\lambda^+ = 30$ and $\lambda^- = 10$ [ev/s], i.e. the same as in Fig. 5.5*d*. Notice the asymmetrical narrow peak on the left side near time zero in the crosscorrelogram. (**b**) Correlation analysis for the pair of units (A, I) with the same parameters as in panel (**a**). (**c**) Firing rate of unit A plotted as λ^- varies, with $\lambda^+ = 10$ ev/s (squares), $\lambda^+ = 20$ ev/s (circles) and $\lambda^+ = 30$ ev/s (diamonds). (**d**) Excitatory efficiency of unit pair (A, E) plotted as λ^- varies, with $\lambda^+ = 10$ ev/s (squares), $\lambda^+ = 20$ ev/s (circles) and $\lambda^+ = 30$ ev/s (diamonds).

generally characterized by mono-aminergic and cholinergic projections from the brainstem to the forebrain could play the role of setting the global parameters. Then, one same neuron could participate to different cell assemblies, characterized by the synchronous firing of many cells, if its firing pattern would include multiple characteristic times.

In this study we analyze two cases of counting processes that give the times of occurrence of the strong inhibitory and excitatory inputs. In the case of Inverse Gaussian (IG) inter events distribution the inputs are very regular in time. Conversely, in the case of Exponentially distributed inter events the strong inputs follow the more casual probabilistic law. As shown by the results of Subsection 5.1.2, the strong inputs that follow an IG distribution dominate the dynamics of the spike train of the target unit A. The IG distribution of the inputs determines the position, shape and number of the peaks appearing in the ISIs histograms of unit A. An increase in the value of the variances $\sigma_+^2 = \sigma_-^2$ of the IG distributions provokes a decrease in the regularity of the inputs processes and the histograms become unimodal. We have shown the existence of two regimes of model dynamics, *subthreshold* and *suprathreshold*, that correspond to two domains in the space of the parameters θ and μ (Fig. 5.2). In the suprathreshold regime the characteristic times of firing are no more integer multiples of the mode m of the IG distribution but become a combination between m and the mode of the first passage time of an Ornstein Uhlenbeck process (2.1.11) through the boundary S (i.e. without jumps). In this regime the crosscorrelation analysis has demonstrated that the "excitatory efficiency" of the strong inputs is decreased following an increase of the parameter θ. This result is interesting because this parameter may have a direct biological interpretation. The parameter θ may correspond to the time constant of the cell membrane determined by its resistive and capacitive properties, i.e. $\theta = RC$, where R is the resistance and C the capacitance of the electrical circuit equivalent to the cell membrane. The capacitance C is usually considered constant on a short time scale. Then, a variation of θ may be considered as a change of the resistive properties of the membrane. This means that our neuromimetic model (2.1.15) accounts for a change in the dynamics following a change of the resistance of the cell membrane. In biology, there are several examples of voltage-dependent ion channels that could account for such changes in the resistive properties of the cell membrane [**9**].

In this framework we have investigated the existence of *resonant* like phenomena in our model. One of the most striking effect emerging from the study of non linear random systems

coupled with a deterministic oscillatory term, is the so called stochastic resonance. Such term is usually referred to the existence of an optimal level of noise for a signal detection and transmission. It has been demonstrated that the multimodal ISI distribution obtained from an Ornstein Uhlenbeck process coupled with a deterministic oscillatory input term goes through a maximum as the noise intensity σ^2 increases [**11**], [**57**]. Such maximum appears when the period of the stimulus is close to the mode of the ISI distribution in absence of the modulation, a phenomenon referred to as *time-scale matching*. In this study we have presented evidence that the peaks of the ISI histograms go through a maximum when the noise intensity σ^2 increased (cf. Subsection 5.1.2.3). Our goal was not to find the optimal level of noise. Instead, in both *open* and *closed circuit* instances the results have shown that the neuronal model introduced in the current study is characterized by a non linear dependence of the level of noise that exhibits a "resonance" like behavior. In the case of the *closed circuit* (Fig. 2.4*a*), with reset of the inputs after each firing, the resonance like behavior could be attributed to the intrinsic feedback loop within the circuit. A similar finding in the *open circuit* instance (Fig. 2.4*b*), which is more biologically plausible, calls for a different interpretation. We suggest that in a large neural network the background activity (here represented by the noise intensity) may act as a filter in selecting particular firing patterns, determined by the characteristic times in the ISI histograms.

In the case that strong inputs follow Poisson processes the range of the parameters characteristic of multimodal ISI distributions is smaller than in the IG distributed inputs. This is because with Poisson distributed inputs the dynamics of the membrane potential is due to both jump processes and diffusion process with no domination of one of the processes on the others. With Poisson inputs and with diffusion parameters in subthreshold regime we found evidence of only bimodal ISI distributions with variable tails depending on the parameters, but without any appearance of a third peak. We have shown that the model linearly integrated the inhibitory inputs (Fig. 5.6*c*) but an increase in the rate of the inhibitory inputs provoked an increase in the efficiency of the excitatory inputs (Fig. 5.6*d*). This means that the timing of the spikes of the excitatory inputs carry more information if the rate of inhibition is increased.

To conclude, this study has presented new results that demonstrate that an original jump-diffusion neuromimetic model, precisely described by its mathematical formulation and

despite a number of oversimplifications, is able to suggest interesting hypotheses for the interpretation of experimentally recorded firing patterns. Resonant like phenomena and the increase in excitatory efficiency due to an increase in the rate of inhibitory inputs represent interesting unexpected results that contribute to widen the investigation of neural dynamics. Future studies of the model presented here could extend further the analyses and investigate the effect of mixtures of jump processes, for example with IG distributed excitatory inputs and Poisson distributed inhibitory inputs.

Part 2

Bridge Processes

CHAPTER 6

Multidimensional bridges with application to the integrated brownian motion

Résumé Le chapitre 6 étudie les processus "bridge" associés à un processus de diffusion générique. L'analyse du temps de premier passage d'un processus de diffusion, approché par le temps de premier sortie d'un processus discretisé, laisse une ambiguïté sur la trajectoire exacte entre deux instants de la discrétisation. Le problème peut avoir de très graves conséquences dans l'évaluation de la solution. Pour résoudre ce problème on écrit l'équation stochastique differentielle satisfaite par le processus bridge. On propose deux méthodes alternatives pour trouver une version de la solution dans le cas bidimensionnel. Les méthodes présentées sont illustrées avec l'exemple du processus "Integrated Brownian Motion". Une généralisation de cette approche est indispensable à l'analyse des modèles neuronaux dans une simulation de réseaux de grand taille.

Contents

In this chapter we explain the results obtained on multidimensional bridge processes and collected in the paper [**61**]. A bridge process (also called tied down process [**28**] or pinned

process [**8**]), associated to a diffusion process X, with $X_0 = a$, is the process X conditioned on the event $\{X_{t_1} = b\}$. That is the diffusion process conditioned on the subset of the trajectories that go through the point (t_1, b). In the literature it is possible to find results about Brownian bridge, i.e. the Brownian motion constrained to attain a given state at time t_1, Bessel bridge and bridges of certain Wiener Integrals [**28**], [**31**], [**32**]. A definition of the general Markov bridges is given in [**17**].

Our interest in bridge processes arises from the field of the simulation of first passage time T of a diffusion process through a threshold S. As explained in Chapter 3, the numerical techniques that allow to solve such problems are based on discrete time approximations of the trajectories of the diffusion process, that give the value of the simulated trajectory, $\tilde{X}_{t_i}$, at discretized times, $(t_i)_{i=0}^N$, of the time interval. At each step the simulated point of the trajectory is compared with the threshold, i.e. $\tilde{X}_{t_i} \leq S$, and the crossing checked. Those techniques may lead to an overestimation of the first passage time. Indeed the crossing may occur at times that lie in between two of the nodes of the partition, $T \in (t_i, t_{i+1})$, so that in correspondence of such times the value of the trajectory has not been calculated. To evaluate the possibility of crossings hidden in between the nodes of the time discretization, in [**21**] the authors introduced an improvement of the algorithm with study of the bridge processes. So that the probability that the bridge process associated to the simulated diffusion process, originated in $(t_i, \tilde{X}_{t_i})$ and constrained to attain the simulated point $(t_{i+1}, \tilde{X}_{t_{i+1}})$, crosses the threshold S is evaluated and compared with a number Uniformly distributed in $[0, 1]$ in order to decide wether the crossing occurred or not. In this way the algorithm accounts for possible crossings at times in between two simulated points of the sample path. In this framework it is particularly important to have results and general techniques that can allow to handle bridge processes. Indeed new results on bridge processes (in particular multidimensional ones) could be applied everywhere the simulation of a first passage time is required. A very interesting field in which those techniques could find a proper application is the simulation of large network of spiking neurons. There it seems very important to correct the algorithm to simulate the firing of each single cell. If not, due to the very large number of repetitions, the final error could go out of control. But this is not the only field in which first passage time problems arise. Let us think to the methods of domain decomposition for elliptic boundary value problems (cf. [**4**] and [**5**]). There, to split the problem into fully decoupled subproblems

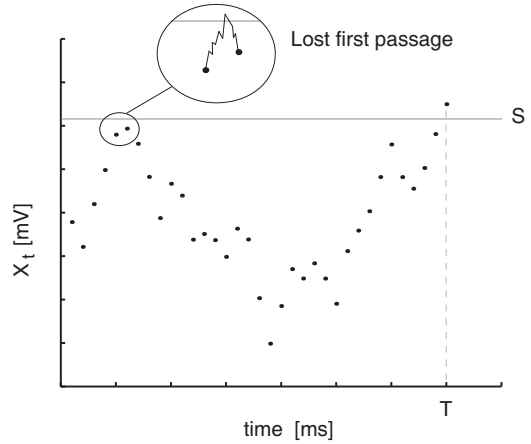

FIGURE 6.1. First passage time T (cf. eq. (2.1.2)) through the constant threshold S of a time discrete approximated sample path of a general diffusion process $X = \{X_t,\ t \geq 0\}$. In the expanded panel a possible trajectory of the process in between two nodes of the discretization of time and the lost first passage time.

on subdomains, first passage times through the boundaries of the decomposed domains need to be found.

In Section 6.2 we introduce a definition of the bridge process associated to a multidimensional diffusion process and we determine the corresponding diffusion coefficients. We apply the result to the case of an Integrated Brownian Motion (IBM) (cf. [**32**]) giving the closed form expression of the solution of the stochastic differential equation (SDE) fulfilled by the IBM bridge. In Section 6.3 we propose two alternative methods to find a version of the solution of the SDE fulfilled by the bridge process in the bidimensional case. The first method looks for space-time transformations that allow to change the solution of the SDE fulfilled by the non conditioned process into a version of the solution of the SDE fulfilled by the associated bridge process. The second method gives the finite dimensional distributions of the bridge process conditioning in a suitable way the solution of an appropriate second order SDE with Dirichlet boundary conditions [**41**] and [**42**]. The methods presented throughout this Section are illustrated via the IBM process.

6.1. Mathematical Background and Notations

Let $X = \{X_t, t \geq 0\}$ be a d-dimensional diffusion process defined on the probability space $(\Omega, \mathcal{F}, (\mathcal{F}_t)_{t\geq 0}, \mathbb{P})$ with state space $\mathbb{R}^d$ satisfying the stochastic differential equation (SDE)

$$\begin{aligned} dX_t &= \mu(t, X_t)dt + \sigma(t, X_t)dW_t \\ X_0 &= c \end{aligned} \tag{6.1.1}$$

where $\{W_t, t \geq 0\}$ is a m-dimensional Wiener process, $\mu : [0, +\infty) \times \mathbb{R}^d \to \mathbb{R}^d$ and $\sigma : [0, +\infty) \times \mathbb{R}^d \to \mathbb{R}^d \times \mathbb{R}^m$ are assumed to be defined and measurable, and $c \in \mathbb{R}^d$. Let us assume that the diffusion coefficients μ and σ satisfy the conditions of existence and uniqueness (cf. [**7**] and [**27**]) of a strong solution of the SDE (6.1.1). For $x, y \in \mathbb{R}^d$ and $s < t \in [0, +\infty)$, let

$$f(x, t|y, s) = \frac{\partial}{\partial x}\mathbb{P}(X_t \leq x|X_s = y) \tag{6.1.2}$$

be the transition probability density function (p.d.f.) of the process X. The p.d.f. is a fundamental solution of the backward Kolmogorov equation, i.e. for fixed $x \in \mathbb{R}^d$, $t \in [0, +\infty)$ and for all $y \in \mathbb{R}^d$ and $s \in [0, +\infty)$ and $s < t$

$$\frac{\partial f(x, t|y, s)}{\partial s} + \sum_{i=1}^{d} \mu_i(s, y)\frac{\partial f(x, t|y, s)}{\partial y_i} + \frac{1}{2}\sum_{i=1}^{d}\sum_{k=1}^{d} \alpha_{ik}(s, y)\frac{\partial^2 f(x, t|y, s)}{\partial y_i \partial y_k} = 0 \tag{6.1.3}$$

and, for fixed $x, y \in \mathbb{R}^d$, satisfies the end condition

$$\lim_{s\uparrow t} f(x, t|y, s) = \delta(x - y) \tag{6.1.4}$$

where δ is Dirac's delta function, μ_i are the components of the vector μ and α_{ik} are the elements of the matrix $\alpha = \sigma\sigma^T$ where T indicates the transpose matrix. The process X, solution of eq. (6.1.1) is called time homogeneous if $\forall x \in \mathbb{R}^d$ the infinitesimal coefficients $\mu(t, x) = \mu(x)$ and $\sigma(t, x) = \sigma(x)$ are independent of time. The process X with state space $I \subseteq \mathbb{R}^d$ is regular if, whenever $x, y \in \overset{\circ}{I}$ (the interior of I)

$$\mathbb{P}(T(y) < \infty|X_0 = x) > 0, \tag{6.1.5}$$

where $T(y)$ is the random variable equal to the first time the process attains the value y (cf. [**28**]).

6.2. Multidimensional bridges

Here we consider the multidimensional bridge associated to a regular time homogeneous diffusion process X, i.e. the process conditioned to attain a given state at time $t_1 > 0$. Our goal is to derive the SDE verified by the conditioned process when is assigned the process X and the corresponding SDE. The case of the Integrated Brownian Motion exemplifies our results.

DEFINITION 6.2.1. Let X be a time homogeneous regular diffusion process. The process $\tilde{X} = \{\tilde{X}_t, 0 \leq t < t_1\}$ is called bridge (or tied-down process) associated to the process X if $\tilde{X}$ is the process X conditioned on $X_{t_1} = b \in \mathbb{R}^d$.

Note that $\tilde{X}$ is a diffusion process itself. In fact it has continuous paths and it is a Markov process (cf. [**28**]).

PROPOSITION 6.2.2. *For $x, y \in \mathbb{R}^d$ and $s < t \in [0, t_1)$ let $\tilde{f}(x, t|y, s)$ be the transition p.d.f. of the conditioned process $\tilde{X}$. The following relation holds*

$$\tilde{f}(x, t|y, s) = \frac{f(x, t|y, s) f(b, t_1|x, t)}{f(b, t_1|y, s)}, \quad s < t \in [0, t_1). \tag{6.2.1}$$

PROOF. Extending the proof given in [**28**] to the case of a general multidimensional regular and time homogeneous diffusion process, for $x, y \in \mathbb{R}^d$ and $s < t \in [0, t_1)$, we get

$$\begin{aligned} \int_A \tilde{f}(x, t|y, s) dx &= \mathbb{P}(X_t \in A | X_{t_1} = b, X_s = y) \\ &= \lim_{\varepsilon \downarrow 0} \mathbb{P}(X_t \in A | X_{t_1} \in \mathcal{B}_b(\varepsilon), X_s = y) \\ &= \lim_{\varepsilon \downarrow 0} \int_A \frac{f(x, t|y, s) \pi(x, t)}{\pi(y, s)} dx \end{aligned} \tag{6.2.2}$$

where $\mathcal{B}_b(\varepsilon)$ is the d-dimensional ball centered in b of radius ε, and for $x \in \mathbb{R}^d$ and $t \in [0, t_1)$, $\pi(x, t)$ is the probability that from the state value x at time t the sample path of X satisfies $X_{t_1} \in \mathcal{B}_b(\varepsilon)$. Hence

$$\int_A \tilde{f}(x, t|y, s) dx = \int_A f(x, t|y, s) \lim_{\varepsilon \downarrow 0} \frac{\int_{\mathcal{B}_b(\varepsilon)} f(z, t_1|x, t) dz}{\int_{\mathcal{B}_b(\varepsilon)} f(z, t_1|y, s) dz} dx, \tag{6.2.3}$$

and we get the thesis. □

Use of (6.2.1) allows to relate the diffusion coefficients of the bridge with the diffusion coefficients and the transition p.d.f. of the not conditioned process. Indeed it holds:

PROPOSITION 6.2.3. *Let X be a d-dimensional regular and time homogeneous diffusion process with infinitesimal coefficients $\mu = \mu(x)$ and $\sigma = \sigma(x)$. The corresponding bridge $\tilde{X}$, obtained conditioning on $X_{t_1} = b$, for $t \in [0, t_1)$, satisfies the following SDE*

$$\begin{aligned} d\tilde{X}_t &= \tilde{\mu}(t, \tilde{X}_t)dt + \tilde{\sigma}(\tilde{X}_t)dW_t \\ \tilde{X}_0 &= c \end{aligned} \tag{6.2.4}$$

where, for $t \in [0, t_1)$ and $x \in \mathbb{R}^d$,

$$\begin{aligned} \tilde{\mu}(t,x) &= \left(\mu_i(x) + \frac{1}{2}\sum_{k=1}^{d} \frac{\alpha_{ik}(x) + \alpha_{ki}(x)}{f(b, t_1|x, t)} \frac{\partial}{\partial x_k} f(b, t_1|x, t)\right)_i \\ \tilde{\sigma}(x) &= \sigma(x) \end{aligned} \tag{6.2.5}$$

PROOF. The transition p.d.f. $f(x, t|y, s)$ of the process X satisfies the backward Kolmogorov equation (6.1.3). From (6.2.1) we have

$$f(x, t|y, s) = \frac{\tilde{f}(x, t|y, s) f(b, t_1|y, s)}{f(b, t_1|x, t)}, \quad s < t \in [0, t_1). \tag{6.2.6}$$

and substituting it into (6.1.3) we obtain

$$\begin{aligned} \frac{\partial \tilde{f}(x, t|y, s)}{\partial s} &+ \sum_{i=1}^{d} \frac{\partial \tilde{f}(x, t|y, s)}{\partial y_i} \left[\mu_i(y) + \frac{1}{2}\sum_{k=1}^{d} \frac{\alpha_{ik}(y) + \alpha_{ki}(y)}{f(b, t_1|x, t)} \frac{\partial}{\partial y_k} f(b, t_1|x, t)\right] \\ &+ \frac{1}{2}\sum_{i=1}^{d}\sum_{k=1}^{d} \alpha_{ik}(y) \frac{\partial^2 \tilde{f}(x, t|y, s)}{\partial y_i \partial y_k} = 0 \end{aligned} \tag{6.2.7}$$

Since the Kolmogorov equation uniquely identifies a diffusion process in terms of the infinitesimal coefficients, the thesis holds. □

REMARK 6.2.4. Note that the infinitesimal variance $\tilde{\sigma}$ of the bridge process $\tilde{X}$ is equal to the infinitesimal variance of the not conditioned process X. On the other hand the drift term $\tilde{\mu}$ changes following equation (6.2.5). Observe that it can be rewritten as

$$\tilde{\mu}(t,x) = \left(\mu_i(x) + \frac{1}{2}\sum_{k=1}^{d} [\alpha_{ik}(x) + \alpha_{ki}(x)] \frac{\partial}{\partial x_k} \ln f(b, t_1|x, t)\right)_i. \tag{6.2.8}$$

Note that if X is solution of a linear SDE then even the corresponding bridge process $\tilde{X}$ is solution of a linear SDE.

REMARK 6.2.5. When eq. (6.2.4) cannot be solved in closed form, it is possible to obtain an approximated solution extending to the multidimensional case the nested algorithm illustrated in [**21**].

6.2.1. Application to the Integrated Brownian Motion.

In this subsection we apply the results obtained in the previous section to the Integrated Brownian Motion process. The process $Z = \{Z_t = (Z_t^{(1)}, Z_t^{(2)})^T, t \geq 0\}$ defined on the probability space $(\Omega, \mathcal{F}, (\mathcal{F}_t)_{t\geq 0}, \mathbb{P})$ with state space $\mathbb{R}^d$ satisfying the following bidimensional stochastic differential equation

$$\begin{cases} dZ_t^{(1)} &= Z_t^{(2)} dt \\ dZ_t^{(2)} &= dW_t \end{cases} \tag{6.2.9}$$

with initial conditions $Z_0^{(1)} = c_1$ and $Z_0^{(2)} = c_2$, where $\{W_t, t \geq 0\}$ is a bidimensional Wiener process, is called Integrated Brownian Motion. Eq. (6.2.9) can be written in matrix form as

$$\begin{aligned} dZ_t &= AZ_t dt + \sigma dW_t \\ Z_0 &= c, \end{aligned} \tag{6.2.10}$$

where $c = (c_1, c_2) \in \mathbb{R}^2$ and A and B are given by

$$A = \begin{pmatrix} 0 & 1 \\ 0 & 0 \end{pmatrix} \qquad \sigma = \begin{pmatrix} 0 & 0 \\ 0 & 1 \end{pmatrix} \tag{6.2.11}$$

Note that eq. (6.2.9) is very simple and the solution is given by

$$\begin{cases} Z_t^{(1)} &= c_1 + c_2 t + \int_0^t W_s ds \\ Z_t^{(2)} &= c_2 + W_t \end{cases} \tag{6.2.12}$$

It results that Z is a bidimensional Gaussian process with mean vector and covariance matrix given by

$$\mathbb{E}(Z_t) = \begin{pmatrix} c_1 + c_2 t \\ c_2 \end{pmatrix} \qquad \mathrm{Cov}(Z_t^{(1)}, Z_t^{(2)}) = \begin{pmatrix} t^3/3 & t^2/2 \\ t^2/2 & t \end{pmatrix} \tag{6.2.13}$$

and the transition p.d.f. for any $z = (z_1, z_2) \in \mathbb{R}^2$ and $t > 0$ is given by

$$\begin{aligned} f_Z(z,t|0,0) &= \frac{\sqrt{3}}{\pi t^2}\exp\left(-\frac{6}{t^3}\left[(z_1-c_1-c_2t)^2+\right.\right. \\ &\quad \left.\left.-t(z_2-c_2)(z_1-c_1-c_2t)+\frac{t^2}{3}(z_2-c_2)^2\right]\right). \end{aligned} \tag{6.2.14}$$

Let us denote with $\tilde{Z}$ the bridge corresponding to the IBM conditioned on being at state $b = (b_1, b_2)$ at time $t_1 = 1$. Applying Proposition 6.2.3 to the IBM process we obtain that the infinitesimal coefficients of the process $\tilde{Z}$, for any $z \in \mathbb{R}^2$ and $t \in [0, 1)$, are

$$\begin{aligned} \tilde{\mu}(t,z) &= \begin{pmatrix} z_2 \\ \\ \dfrac{6(b_1-z_1)}{(1-t)^2} - \dfrac{2(2z_2+b_2)}{(1-t)} \end{pmatrix} \\ \tilde{\sigma}(z) &= \begin{pmatrix} 0 & 0 \\ 0 & 1 \end{pmatrix} \end{aligned} \tag{6.2.15}$$

Hence the linear SDE fulfilled by the process $\tilde{Z}$ can be written in matrix form for $t \in [0, 1)$ as follows

$$\begin{aligned} d\tilde{Z}_t &= [\tilde{A}(t)\tilde{Z}_t + \tilde{a}(t)]dt + \tilde{\sigma}dW_t \\ \tilde{Z}_0 &= c, \end{aligned} \tag{6.2.16}$$

where $\tilde{\sigma}$ is as in eq. (6.2.15) and $\tilde{A}$ and $\tilde{a}$ are given by

$$\tilde{A} = \begin{pmatrix} 0 & 1 \\ \\ \dfrac{-6}{(1-t)^2} & \dfrac{-4}{(1-t)} \end{pmatrix} \qquad \tilde{a} = \begin{pmatrix} 0 \\ \\ \dfrac{6b_1}{(1-t)^2} - \dfrac{2b_2}{(1-t)} \end{pmatrix} \tag{6.2.17}$$

The solution of eq. (6.2.16) is given by

$$\tilde{Z}_t = \Phi(t)\left[c + \int_0^t \Phi^{-1}(s)\tilde{a}(s)ds + \int_0^t \Phi^{-1}(s)\tilde{\sigma}dW_s\right], \quad 0 \le t < 1 \tag{6.2.18}$$

where the matrix function $\Phi(t)$ is the fundamental solution to the homogeneous equation $\dot{x}(t) = \tilde{A}(t)x(t)$ (cf. [**22**]). After some calculation we obtain that

$$\Phi(t) = \begin{pmatrix} (2t+1)(t-1)^2 & t(t-1)^2 \\ \\ 6t(t-1) & (t-1)(3t-1) \end{pmatrix} \tag{6.2.19}$$

and the solution of eq. 6.2.16 is

$$\begin{cases} \tilde{Z}_t^{(1)} &= c_1(2t+1)(t-1)^2 + c_2 t(t-1)^2 + b_1 t^2(3-2t) + b_2 t^2(t-1) + \\ & \quad -(t-1)^2 \displaystyle\int_0^t \frac{s}{(s-1)^2} dW_s + t(t-1)^2 \int_0^t \frac{1}{(s-1)^2} dW_s \\ \\ \tilde{Z}_t^{(2)} &= 6c_1 t(t-1) + c_2(3t-1)(t-1) + 6b_1 t(1-t) + b_2 t(3t-2) + \\ & \quad -2(t-1) \displaystyle\int_0^t \frac{s}{(s-1)^2} dW_s + (t-1)(3t-1) \int_0^t \frac{1}{(s-1)^2} dW_s \end{cases}$$

Note that $\tilde{Z}$ is a Gaussian process with vector mean and covariance function $\mathrm{Cov}(\tilde{Z}_t, \tilde{Z}_s) = \mathbb{E}[(\tilde{Z}_t - \mathbb{E}(\tilde{Z}_t))(\tilde{Z}_s - \mathbb{E}(\tilde{Z}_s))^T]$ given by

$$\begin{aligned} \mathbb{E}(\tilde{Z}_t) &= \begin{pmatrix} c_1(2t+1)(t-1)^2 + c_2 t(t-1)^2 + b_1 t^2(3-2t) + b_2 t^2(t-1) \\ \\ 6c_1 t(t-1) + c_2(3t-1)(t-1) + 6b_1 t(1-t) + b_2 t(3t-2) \end{pmatrix} \\ \mathrm{Cov}(\tilde{Z}_t, \tilde{Z}_s) &= \begin{pmatrix} s^2(1-t)^2 \left[-\dfrac{s(1-t)}{6} + \dfrac{t(1-s)}{2} \right] & \dfrac{s(1-t)^2}{2}(2st+s-2t) \\ \\ \dfrac{t(1-s)^2}{2}(2st+t-2s) & s(1-t)(3st+1-3t) \end{pmatrix} \end{aligned} \tag{6.2.20}$$

6.3. Two methods to find a version of the bridge process in the bidimensional case

In this section we present two different methods to calculate the distribution of a bridge associated to a given bidimensional diffusion process. The first method looks for time-space transformations that allow to obtain a version of the process solution of the SDE for the bridge knowing the solution of the SDE of the not conditioned process, following a method proposed in [**47**] for a similar one dimensional problem. The second method allows to obtain

the distribution of the bridge by conditioning the second component of the process solution of a second order SDE with Dirichlet boundary conditions (cf. [**42**]).

6.3.1. Space-time transformation of the process. In this subsection we look for space-time transformations (cf. [**13**],[**47**]) of the type

$$\begin{aligned} s' &= \phi(s) \\ y_1' &= \psi_1(s, y_1, y_2) \\ y_2' &= \psi_2(s, y_1, y_2) \end{aligned} \tag{6.3.1}$$

with the further condition

$$f(x, t|y, s) = Jf'(x', t'|y', s') \tag{6.3.2}$$

where $s > 0$, $s' \in [0, t_1)$, $y = (y_1, y_2)^T \in \mathbb{R}^2$, $y' = (y_1', y_2')^T \in \mathbb{R}^2$ and J is the Jacobian of the transformation. Equations (6.3.1) and (6.3.2) change eq. (6.1.3) into the Kolmogorov equation of the bridge corresponding to the original process that is eq. (6.2.7) for $d = 2$. Rewriting eq. (6.1.3) in terms of the new variables given by (6.3.1) and equating it to the new Kolmogorov equation given by eq. (6.2.7) for $d = 2$, we obtain the following system of

partial differential equations:

$$
\begin{cases}
\dfrac{\partial\psi_1(s,y)}{\partial s}+\mu_1(y)\dfrac{\partial\psi_1(s,y)}{\partial y_1}+\mu_2(y)\dfrac{\partial\psi_1(s,y)}{\partial y_2}+\dfrac{a_{11}(y)}{2}\dfrac{\partial^2\psi_1(s,y)}{\partial y_1^2}+ \\
\quad+\dfrac{a_{22}(y)}{2}\dfrac{\partial^2\psi_1(s,y)}{\partial y_2^2}+\dfrac{a_{12}(y)+a_{21}(y)}{2}\dfrac{\partial^2\psi_1(s,y)}{\partial y_1\partial y_2}=\tilde{\mu}_1(\phi(s),\psi(s,y))\dfrac{d\phi(s)}{ds} \\
\dfrac{\partial\psi_2(s,y)}{\partial s}+\mu_1(y)\dfrac{\partial\psi_2(s,y)}{\partial y_1}+\mu_2(y)\dfrac{\partial\psi_2(s,y)}{\partial y_2}+\dfrac{a_{11}(y)}{2}\dfrac{\partial^2\psi_2(s,y)}{\partial y_1^2}+ \\
\quad+\dfrac{a_{22}(y)}{2}\dfrac{\partial^2\psi_2(s,y)}{\partial y_2^2}+\dfrac{a_{12}(y)+a_{21}(y)}{2}\dfrac{\partial^2\psi_2(s,y)}{\partial y_1\partial y_2}=\tilde{\mu}_2(\phi(s),\psi(s,y))\dfrac{d\phi(s)}{ds} \\
a_{11}(y)\left(\dfrac{\partial\psi_1(s,y)}{\partial y_1}\right)^2+a_{22}(y)\left(\dfrac{\partial\psi_1(s,y)}{\partial y_2}\right)^2+(a_{12}(y)+a_{21}(y))\dfrac{\partial\psi_1(s,y)}{\partial y_1}\dfrac{\partial\psi_1}{\partial y_2}= \\
\quad=a_{11}(\psi(s,y))\dfrac{d\phi(s)}{ds} \\
a_{11}(y)\left(\dfrac{\partial\psi_2(s,y)}{\partial y_1}\right)^2+a_{22}(y)\left(\dfrac{\partial\psi_2(s,y)}{\partial y_2}\right)^2+(a_{12}(y)+a_{21}(y))\dfrac{\partial\psi_2(s,y)}{\partial y_1}\dfrac{\partial\psi_2(s,y)}{\partial y_2}= \\
\quad=a_{22}(\psi(s,y))\dfrac{d\phi(s)}{ds} \\
2a_{11}(y)\dfrac{\partial\psi_1(s,y)}{\partial y_1}\dfrac{\partial\psi_2(s,y)}{\partial y_1}+2a_{22}(y)\dfrac{\partial\psi_1(s,y)}{\partial y_2}\dfrac{\partial\psi_2(s,y)}{\partial y_2}+ \\
\quad+2(a_{12}(y)+a_{21}(y))\dfrac{\partial\psi_1(s,y)}{\partial y_1}\dfrac{\partial\psi_2(s,y)}{\partial y_2}=(a_{12}(y)+a_{21}(y))\dfrac{d\phi(s)}{ds}
\end{cases}
\tag{6.3.3}
$$

where $\psi(s,y) = (\psi_1(s,y), \psi_2(s,y))^T$, with the conditions

$$\begin{aligned}
&\phi(0) = 0 \\
&\lim_{s\to\infty} \phi(s) = t_1 \\
&\psi_1(0, c_1, c_2) = c_1 \\
&\psi_2(0, c_1, c_2) = c_2 \\
&\lim_{s\to\infty} \psi_1(s, y_1, y_2) = b_1, \qquad \forall y \in \mathbb{R}^2 \\
&\lim_{s\to\infty} \psi_2(s, y_1, y_2) = b_2, \qquad \forall y \in \mathbb{R}^2.
\end{aligned} \tag{6.3.4}$$

In the general case the system (6.3.3) is not solvable in closed form. Hence we focus on the particular case of the IBM process.

Application to the IBM process. Let us consider the process Z given by eq. (6.2.9). We look for the transformations that allows to change the Kolmogorov equation for the IBM transition p.d.f.

$$\frac{\partial f}{\partial s} + y_2 \frac{\partial f}{\partial y_1} + \frac{1}{2}\frac{\partial^2 f}{\partial y_2^2} = 0 \tag{6.3.5}$$

into the Kolmogorov equation for the transition p.d.f. of the corresponding bridge $\tilde{Z}$, given by

$$\frac{\partial f'}{\partial s'} + y_2' \frac{\partial f'}{\partial y_1'} + \left[\frac{6(b_1 - y_1')}{(1-t')^2} - \frac{2(2y_2' + b_2)}{(1-t')}\right] \frac{\partial f'}{\partial y_2'} + \frac{1}{2}\frac{\partial^2 f'}{\partial y_2'^2} = 0 \tag{6.3.6}$$

obtained substituting (6.2.15) in eq. (6.2.7). When considering an IBM bridge, the system (6.3.3) becomes

$$\begin{cases} \dfrac{\partial\psi_1(s,y)}{\partial s} + y_2\dfrac{\partial\psi_1(s,y)}{\partial y_1} + \dfrac{1}{2}\dfrac{\partial^2\psi_1(s,y)}{\partial y_2^2} = \psi_2(s,y)\dfrac{d\phi(s)}{ds} \\ \dfrac{\partial\psi_2(s,y)}{\partial s} + y_2\dfrac{\partial\psi_2(s,y)}{\partial y_1} + \dfrac{1}{2}\dfrac{\partial^2\psi_2(s,y)}{\partial y_2^2} = \dfrac{d\phi(s)}{ds}\left[\dfrac{6(b_1-\psi_1(s,y))}{(1-\phi(t))^2} - \dfrac{2(2\psi_2(s,y)+b_2)}{(1-\psi(t))}\right] \\ \left(\dfrac{\partial\psi_1(s,y)}{\partial y_2}\right)^2 = 0 \\ \left(\dfrac{\partial\psi_2(s,y)}{\partial y_2}\right)^2 = \dfrac{d\phi(s)}{ds} \\ 2\dfrac{\partial\psi_1(s,y)}{\partial y_2}\dfrac{\partial\psi_2(s,y)}{\partial y_2} = 0 \end{cases} \tag{6.3.7}$$

with conditions (6.3.4). The system (6.3.7) has infinite solutions, one for each choice of the function $\phi(t)$ satisfying conditions (6.3.4). Fixing the transformation for the time

$$\phi(s) = \frac{s}{1+s} \tag{6.3.8}$$

we obtain the following transformations for the spaces

$$\begin{aligned} \psi_1(s,y_1,y_2) &= \frac{y_1 - b_2 + 2b_1 - 3c_1}{(s+1)^3} + \frac{b_1 s^2 + (1-s)(b_2-2b_1) + 3c_1}{(s+1)^2} \\ \psi_2(s,y_1,y_2) &= \frac{y_2 - 3b_2 + b_2 t + 4b_1 - 6c_1}{(s+1)} + \frac{-3y_1 + 3(b_2-2b_1) + 9c_1}{(s+1)^2}. \end{aligned} \tag{6.3.9}$$

Then, applying the previous transformations to the solution (6.2.12), we find that a version of the IBM bridge is given by the process $\bar{Z}$ as follows

$$\begin{cases} \bar{Z}_t^{(1)} &= c_1(2t+1)(t-1)^2 + c_2 t(t-1)^2 + b_1 t^2(3-2t) + b_2 t^2(t-1) + \\ &\quad -(t-1)^3\displaystyle\int_0^{t/(1-t)} W_s ds \\ \bar{Z}_t^{(2)} &= 6c_1 t(t-1) + c_2(3t-1)(t-1) + 6b_1 t(1-t) + b_2 t(3t-2) + \\ &\quad -(t-1)W_{\frac{t}{(1-t)}} - 3(1-t)^2\displaystyle\int_0^{t/(1-t)} W_s ds \end{cases}$$

Simple computations allows to see that the process $\bar{Z}$ has the same finite-dimensional distributions as process $\tilde{Z}$.

6.3.2. Second order SDE with Dirichlet boundary conditions. In this subsection we consider the particular case of a one-dimensional diffusion process $Y = \{Y_t, t \in [0, t_1)\}$ fulfilling the following second order SDE

$$\frac{d^2Y_t}{dt^2} + f\left(Y_t, \frac{dY_t}{dt}\right) = \frac{dW_t}{dt}, \tag{6.3.10}$$

with Dirichlet type boundary conditions

$$Y_0 = c_1 \quad Y_{t_1} = b_1 \tag{6.3.11}$$

where c_1 and b_1 are real fixed numbers. Note that the solution of eq. (6.3.10) with boundary conditions (6.3.11) is a process originated in c_1 and constrained to be at time t_1 in state b_1. If we also condition the derivative of the process to attain a fixed value at time $t = 0$ and $t = t_1$ we get a process equal in law to a bridge. In fact if we consider the bidimensional process $\hat{Y}_t = (\hat{Y}_t^{(1)} = Y_t, \hat{Y}_t^{(2)} = dY_t/dt)$, eq. (6.3.10) can be written as

$$\left\{ \begin{array}{rcl} d\hat{Y}_t^{(1)} & = & \hat{Y}_t^{(2)} dt \\ d\hat{Y}_t^{(2)} & = & -f(\hat{Y}_t^{(1)}, \hat{Y}_t^{(2)})dt + dW_t \end{array} \right. \tag{6.3.12}$$

and with this notation the boundary conditions (6.3.11) are

$$\hat{Y}_0^{(1)} = c_1 \quad \hat{Y}_{t_1}^{(1)} = b_1. \tag{6.3.13}$$

The process $\hat{Y}$ conditioned on the event $B = \{\hat{Y}_0^{(2)} = c_2, \hat{Y}_{t_1}^{(2)} = b_2\}$ becomes a new process $\tilde{Y}$ originated in (c_1, c_2) and constrained to attain value (b_1, b_2) at time t_1. The process $\tilde{Y}$ has the same finite-dimensional distributions of the bridge associated to the process Y.

Application to the IBM process. Let's consider eq. (6.3.10) with boundary conditions (6.3.11) for $f \equiv 0$ and $t_1 = 1$. Denote by $\hat{Z} = (\hat{Z}_t^{(1)} = Z_t, \hat{Z}_t^{(2)} = dZ_t/dt)$ the solution given by

$$\left\{ \begin{array}{rcl} \hat{Z}_t^{(1)} & = & c_1 + (b_1 - c_1)t - t\displaystyle\int_0^1 W_s ds + \int_0^t W_s ds \\ \\ \hat{Z}_t^{(2)} & = & (b_1 - c_1) - \displaystyle\int_0^1 W_s ds \end{array} \right.$$

Note that $\hat{Z}$ is a Gaussian process with vector mean and covariance function given by

$$\begin{aligned} \mathbb{E}(\hat{Z}_t) &= \begin{pmatrix} c_1 + (b_1 - c_1)t \\ \\ (b_1 - c_1) \end{pmatrix} \\ \mathrm{Cov}(\tilde{Z}_t, \tilde{Z}_s) &= \begin{pmatrix} \frac{s(t-1)}{6}[s^2 + t(t-2)] & \frac{(t-1)}{6}[3s^2 + t(t-2)] \\ \\ \frac{(s-1)}{6}[3t^2 + s(s-2)] & \frac{t^2+s^2}{2} - t + \frac{1}{3} \end{pmatrix}, \end{aligned} \tag{6.3.14}$$

for $s < t \in [0, 1)$.

PROPOSITION 6.3.1. *The process $\hat{Z}$ conditioned on the event $B = \{\hat{Z}_0^{(2)} = c_2, \hat{Z}_1^{(2)} = b_2\}$ has the same finite-dimensional distributions of the IBM bridge $\tilde{Z}$ given by eq. (6.2.20).*

PROOF. In order to get the thesis let us calculate the distribution of the conditioned process $\hat{Z}|B$. To this aim let us consider the 4-dimensional Gaussian vector

$$H = \begin{pmatrix} H_1 \\ H_2 \end{pmatrix} \tag{6.3.15}$$

where $H_1 = (\hat{Z}_0^2, \hat{Z}_1^2)^T$ and $H_2 = (\hat{Z}_t^1, \hat{Z}_t^2)^T$. We recall that given

$$X = \begin{pmatrix} X_1 \\ \vdots \\ X_k \\ X_{k+1} \\ \vdots \\ X_n \end{pmatrix} = \begin{pmatrix} X_{(1)} \\ X_{(2)} \end{pmatrix} \tag{6.3.16}$$

a Gaussian n-dimensional vector with vector mean and covariance matrix

$$\begin{aligned} \mathbb{E}(X) &= \begin{pmatrix} \mu_1 \\ \mu_2 \end{pmatrix} \\ \Sigma(X) &= \begin{pmatrix} \Sigma_{11} & \Sigma_{12} \\ \Sigma_{21} & \Sigma_{22} \end{pmatrix}, \end{aligned} \tag{6.3.17}$$

where $\mu_i = \mathbb{E}(X_{(i)})$ and $\Sigma_{ij} = \mathrm{Cov}(X_{(i)}, X_{(j)})$, the distribution of the conditioned process $X_{(2)}|X_{(1)}$ is again Gaussian with mean $\mu_{2|1}$ and covariance matrix $\Sigma_{22|1}$ (cf. [**58**])

$$\begin{aligned} \mu_{2|1} &= \mu_2 + \Sigma_{21}\Sigma_{11}^{-1}(X_{(1)} - \mu_1), \\ \Sigma_{22|1} &= \Sigma_{22} - \Sigma_{21}\Sigma_{11}^{-1}\Sigma_{12}. \end{aligned} \tag{6.3.18}$$

Applying this result to the vector H we get

$$\mathbb{E}(H) = \begin{pmatrix} b_1 - c_1 \\ b_1 - c_1 \\ c_1 + (b_1 - c_1)t \\ b_1 - c_1 \end{pmatrix} \tag{6.3.19}$$

$$\Sigma(H) = \begin{pmatrix} \frac{1}{3} & -\frac{1}{6} & \frac{t}{6}(t-1)(t-2) & \frac{t^2}{2} - t + \frac{1}{3} \\ -\frac{1}{6} & \frac{1}{3} & \frac{t}{6}(t^2-1) & \frac{t^2}{2} - \frac{1}{6} \\ \frac{t}{6}(t-1)(t-2) & \frac{t}{6}(t^2-1) & \frac{t^2}{3}(t-1)^2 & \frac{t}{3}(2t-1)(t-1) \\ \frac{t^2}{2} - t + \frac{1}{3} & \frac{t^2}{2} - \frac{1}{6} & \frac{t}{3}(2t-1)(t-1) & t^2 - t + \frac{1}{3} \end{pmatrix}.$$

Hence the conditioned process $\hat{Z}|B$ at time t is Gaussian distributed with mean vector and covariance matrix given by

$$\mathbb{E}(\hat{Z}_t|B) = \begin{pmatrix} c_1(2t+1)(t-1)^2 + c_2 t(t-1)^2 + b_1 t^2(3-2t) + b_2 t^2(t-1) \\ 6c_1 t(t-1) + c_2(3t-1)(t-1) + 6b_1 t(1-t) + b_2 t(3t-2) \end{pmatrix}$$

$$\mathrm{Cov}(\tilde{Z}_t^{(1)}, \tilde{Z}_t^{(2)}|B) = \begin{pmatrix} \frac{t^3(1-t)^3}{3} & \frac{t^2}{2}(1-2t)(1-t)^2 \\ \frac{t^2}{2}(1-2t)(1-t)^2 & t(1-t)(3t^2-3t+1), \end{pmatrix} \tag{6.3.20}$$

that are equal to (6.2.20) for $s = t$. In order to obtain the covariance function of $\hat{Z}|B$ we apply the same method to the Gaussian vector H with $H_2 = (\hat{Z}^1_t, \hat{Z}^1_s)^T$, $H_2 = (\hat{Z}^1_t, \hat{Z}^2_s)^T$ and $H_2 = (\hat{Z}^2_t, \hat{Z}^2_s)^T$ respectively and we get the thesis. □

6.4. Discussion

In this first study on bridge processes we tried to follow an approach to the problem that goes through the SDE fulfilled by the conditioned process, starting from the SDE giving the process on which the bridge is built. We explored two methods to have a version (at least) of the solution of the SDE giving the bridge, i.e. the space time transformations and the conditioning of the solution of a suitable second order SDE with Dirichlet boundary conditions.

This is truly an explorative study, we are going to complete. At first we would like to build another example to illustrate the results. Then we would like to work on the first passage time of the bridge process through the threshold. Indeed the application of bridge processes in which we are mainly interested, as already said, is the simulation of first passage times of diffusion processes. There we need to have results on the first passage time of the bridge process build on the diffusion process that is simulated. So we consider this (very intriguing) problem still open.

CHAPTER 7

Conclusions

Résumé Le chapitre 7 rappelle le cheminement qui nous a permis de passer des modèles mathématiques simples aux modèles de plus en plus compliqués pour la simulation de la dynamique neuronale. Les principaux résultats obtenus sont rappelés sourtout à la lumière de leur interprétation neurobiologique: premièrement, l'observation qu'une afférence inhibitrice peut renforcer l'efficacité des afférences excitatrices sous certaines conditions; deuxièmement, l'observation des distributions ISI multimodales en l'absence d'afférences périodiques est particulièrment importante dans la perspective des synchronisations de l'activité cerebrale. Le dévelopement ultérieur des résultats de cette thèse, aussi bien dans le domaine des neurosciences computationelles que dans les applications informatiques, est décrit avec quelques exemples.

We developed our studies in two main directions. On one hand, we studied stochastic neuronal models where the membrane potential is described through a jump diffusion process. We showed that, even if simple, such models are able to produce complex and interesting dynamics. We focused our attention on the properties of the firing patterns of a small network consisting in one single neuron and two units (cell assemblies) synapting on it. The investigated features (such as multimodality of the ISIs histograms, resonant like phenomena and correlations) allow to widen the perspective and to set the small network in a larger environment. On the other hand we faced, from a purely theoretical point of view, the study of multidimensional bridge processes associated to a diffusion process. We wrote the SDE fulfilled by the conditioned process, starting from the SDE giving the process on which the bridge is built. We explored two methods to have a version of the solution of the SDE giving the bridge, i.e. the space time transformations and the conditioning of the solution of a suitable second order SDE with Dirichlet boundary conditions.

With respect to the neuromodelling topic we dealt with the following models:

- Wiener process with jumps (2.1.16):
  - N^+ and N^- Poisson processes
  - N^+ and N^- with inter events IG distributed
- Ornstein Uhlenbeck process with jumps (2.1.14):
  - with reset to $V_0^{OU} = V_{rest}$ and $N_0^+ = N_0^- = 0$:
    - N^+ and N^- Poisson processes
    - N^+ and N^- with inter events IG distributed
  - with reset to $V_0^{OU} = V_{rest}$ and $N_0^+ = N_{T_k}^+$ and $N_0^- = N_{T_k}^-$:
    - N^+ and N^- Poisson processes
    - N^+ and N^- with inter events IG distributed

The study of the Wiener process with jumps has been mainly preliminary, and allowed us to introduce and focus the problems we developed more in details with the Ornstein Uhlenbeck process with jumps. The results we obtained show that the superimposition of the jump processes with Inverse Gaussian or Exponential inter events distributions considerably changes the dynamics of the membrane potential. The two jump processes we considered have very different consequences on the dynamics of the membrane potential. When the inter events are Inverse Gaussian distributed, the jump processes force the membrane potential fluctuations with strong regularities (cf. Fig. 5.3, panels *a*–*b*), that we find again in the ISI histograms. While with Exponential distribution of the inter times, the jumps processes have no regular nor oscillatory component (cf. Fig. 5.6, panels *a*–*b*). Despite that, the composition with the jump diffusion process, for some range of the parameters, gives rise to ISI histograms again multimodal. We gave particular relevance to this feature exhibited by the ISI histograms. Indeed to consider firing times of the nerve cell given by a random variable distributed according to a density with multiple peaks, means that in correspondence of each one of the modes (i.e. the lags giving the maxima of the density) the cell has a higher probability of firing (referred to as *characteristic time*). The hypothesis that the probability of firing around a characteristic time could be modulated is confirmed by the study on resonant like phenomena we performed. So that the same single neuron, when varying physiological background properties, may produce firing patterns significantly different and participate to different circuits.

The other relevant results we obtained on the study of the neuromimetic model concerns the role of inhibition in neuronal coding. Indeed we show that inhibition helps the excitatory signal transmission (cf. Fig. 5.6, panel *d*). This result suggests that inhibitory cells are not only involved in keeping a stable balance with excitation but also may take an active role in the information processing. To some extent we could say that the role of inhibitory inputs can be considered "content driven".

Beside the neuro-modelling problem, we worked on bridge processes associated to a diffusion process. We obtained purely theoretical results we would like to apply to first passage time simulation problems. Indeed the algorithms to simulate the first passage time of a stochastic process through a threshold (that is the mathematical formulation we adopted to find the firing times of a neuron with membrane potential modelled through a stochastic process) build time discrete approximations of the sample path of the considered stochastic process and at each step evaluate whether the new point lies beyond the boundary. These procedures cause the loss of possible crossings in between two successive simulated points. We ignore such occurrences since we ignore the trajectory in between two nodes of the time discrete approximation of the trajectory. The error that affects the first passage time estimate is very relevant (cf. [**19**]). So that the algorithm is corrected by adding, at each step, the evaluation of the probability that the bridge process built conditioning on the nodes of the partition of the time crosses the threshold. Note that if we deal with large networks of neurons and we are interested in a simulation of such network, the presence of an important error on each cell will propagate. The study we performed on multidimensional bridges is at an early stage and we are planning to apply them to the simulation of large networks of neurons. Pure mathematical applications of first passage time problems arise also in algorithms that solve elliptic boundary value problems with domain decomposition methods. There, to split the problem into fully decoupled problems, it is important to have efficient and reliable algorithms at disposal to evaluate first passage times.

Bibliography

[1] M. Abeles. Quantification, smoothing and confidence limits for single units' histograms. *J. Neurosci. Meth.*, 5:317–325, 1982.

[2] M. Abeles. *Corticonics: Neural Circuits of the Cerebral Cortex*. Cambridge Univ. Press, New York, 1991.

[3] M. Abeles and G.L. Gerstein. Detecting spatiotemporal firing patterns among simultaneously recorded single neurons. *J. Neurophysiol.*, 60:909–924, 1988.

[4] J. A. Acebrón, M. P. Busico, P. Lanucara, and R. Spigler. Domain decomposition solution of elliptic boundary-value problems via Monte Carlo and quasi-Monte Carlo methods. *SIAM J. Sci. Comput.*, 27(2):440–457, 2005.

[5] J. A. Acebrón, M. P. Busico, P. Lanucara, and R. Spigler. Probabilistically induced domain decomposition methods for elliptic boundary-value problems. *J. Comput. Phys.*, 210(2):421–438, 2005.

[6] A.M.H.J. Aertsen, G.L. Gerstein, M.K. Habib, and Palm G. Dynamics of neuronal firing correlation: modulation of effective connectivity. *J. Neurophysiol.*, 61:900–917, 1989.

[7] L. Arnold. *Stochastic differential equations: theory and applications*. Krieger Publishing Company, Malabar, Florida, 1974.

[8] P. Baldi and L. Caramellino. Asymptotics of hitting probabilities for general one-dimensional pinned diffusions. *Ann. Appl. Probab.*, 12(3):1071–1095, 2002.

[9] F. Benzanilla. The voltage sensor in voltage-dependent ion channels. *Physiol. Rev.*, 80:555–592, 2000.

[10] A. R. Bulsara, S.B. Lowen, and C.D. Rees. Cooperative behavior in the periodically modulated Wiener process: Noise-induced complexity in a model neutron. *Phys. Rev. E*, 49(6):49895000, 1994.

[11] A.R. Bulsara, T. Elston, C. Doering, and S.B. Lowen. Cooperative behavior in the periodically driven noisy integrate-fire models of neuronal dynamics. *Phys. Rev. E*, 53(4):3958–3969, 1996.

[12] R.M. Capocelli and L.M. Ricciardi. Diffusion approximation and first passage time problem for a model neuron. *Kybernetik*, 8:214–223, 1971.

[13] I.D. Cherkasov. On the transformation of the diffusion process to a Wiener process. *Theory Probab. Appl.*, 2:373–377, 1957.

[14] J. del Castillo and B. Katz. Biochemical aspects of neuromuscular transmission. *Progr. Biophys. Biochem.*, 6:121–170, 1956.

[15] J.C. Eccles. *The Physiology of Nerve Cells*. Baltimore, Maryland, Johns Hopkins Press, 1957.

[16] P. Fatt and B. Katz. Spontaneous subthreshold activity at motor nerve endings. *J. Physiol.*, 117:109–128, 1952.

[17] P. Fitzsimmons, J. Pitman, and M. Yor. Markovian bridges: construction, Palm interpretation, and splicing. In *Seminar on Stochastic Processes, 1992 (Seattle, WA, 1992)*, volume 33 of *Progr. Probab.*, pages 101–134. Birkhäuser Boston, Boston, MA, 1993.

[18] G.L. Gerstein and B. Mandelbrot. Random walk models for the spike activity of a single neuron. *Biophys. J.*, 4:41–67, 1964.

[19] M.T. Giraudo and L. Sacerdote. An improved technique for the simulation of first passage times for diffusion processes. *Statist. Simula.*, 28(4):1135–1163, 1999.

[20] M.T. Giraudo, L. Sacerdote, and R. Sirovich. Effects of random jumps on a very simple neuronal diffusion model. *BioSystems*, 67:75–83, 2002.

[21] M.T Giraudo, L. Sacerdote, and C. Zucca. A Monte Carlo method for the simulation of first passage times of diffusion processes. *Methodology and Computing in Appl Probab*, 3:215–231, 2001.

[22] J.K. Hale. *Ordinary differential equations*. John Wiley & Sons, New York, 1969.

[23] D.O. Hebb. *The organization of behavior*. Wiley, New York, 1949.

[24] A. L. Hogkin and A. F. Huxley. A quantitative description of membrane current and its application to conduction and excitation in nerve. . *Physiol.*, 117:500–44, 1952d.

[25] G. Kallianpur. On the diffusion approximation to a discontinuous model for a single neuron. *Contributions to Statistics (P. K. Sen, ed.)*, 1983.

[26] G. Kallianpur and R.L. Wolpert. Weak convergence of stochastic neuronal models. *Stochastic methods in biology, Lect. Notes Biomath.*, 70, 1987.

[27] I. Karatzas and S.E. Shreve. *Brownian motion and stochastic calculus*, volume 113 of *Graduate Texts in Mathematics*. Springer-Verlag, New York, second edition, 1991.

[28] S. Karlin and H.M. Taylor. *A second course in stochastic processes*. Academic Press Inc. [Harcourt Brace Jovanovich Publishers], New York, 1981.

[29] A.Y. Khintchine. *Mathematical methods in the theory of queueing*. Translated by D. M. Andrews and M. H. Quenouille. Griffin's Statistical Monographs & Courses, No. 7. Hafner Publishing Co., New York, 1960.

[30] P.E. Kloeden and E. Platen. *Numerical solution of stochastic differential equations*, volume 23 of *Applications of Mathematics (New York)*. Springer-Verlag, Berlin, 1992.

[31] A. Lachal. Bridges of certain Wiener Integrals. prediction properties, relation with polynomial interpolation and differential equations. application to goodness-of-fit testing. *Bolyai Society Mathematical Studies, X. Limit Theorems, Balatonlelle (Hungary), 1999. Budapest, 2002*, pages 1–51.

[32] A. Lachal. *Etude des Trajectoires de la Primitive du Mouvement Brownien*. Thèse de doctorat en mathematiques, Université Claude Bernard Lyon, 1992.

[33] P. Lánský. On approximations of Stein's neuronal model. *J. Theor. Biol.*, 107:631–647, 1984.

[34] M. London and I. Segev. Synaptic scaling *in vitro* and *in vivo*. *Nat. Neurosci.*, 4(9):853–855, 2001.

[35] A. Longtin, A. Bulsara, and F. Moss. Time interval sequences in the bistable systems and the noise induced transmission of information by sensory neurons. *Phys. Rev. Lett.*, 67:656, 1991.

[36] J.C. Magee. Dendritic integration of excitatory synaptic input. *Nat. Rev. Neurosci.*, 1:181–190, 2000.

[37] J.C. Magee and E.P. Cook. Somatic EPSP amplitude is independent of synapse location in hippocampal pyramidal neurons. *Nat. Neurosci.*, 3:895–903, 2000.

[38] R. Michael, W.R. Schucany, and R.W. Haas. Generating random variates using transformations with multiple roots. *The American Statistician*, 30(2):88–90, 1976.

[39] F. Moss, A. Bulsara, and M.F. Shlesinger. Proceedings of the NATO advanced research workshop on stochastic resonance in physics and biology. *J. Stat. Phys.*, 1993.

[40] M. Musila and P. Lánský. Generalized Stein's model for anatomically complex neurons. *BioSystems*, 25:179–191, 1991.

[41] D. Nualart and É. Pardoux. Boundary value problems for stochastic differential equations. *Ann. Probab.*, 19(3):1118–1144, 1991.

[42] D. Nualart and É. Pardoux. Second order stochastic differential equations with Dirichlet boundary conditions. *Stochastic Process. Appl.*, 39(1):1–24, 1991.

[43] D.H. Perkel, G.L. Gerstein, and G.P. Moore. Neuronal spike trains and stochastic point processes i. *Biophys. J.*, 7:391–418, 1967a.

[44] D.H. Perkel, G.L. Gerstein, and G.P. Moore. Neuronal spike trains and stochastic point processes i. *Biophys. J.*, 7:419–440, 1967b.

[45] W. Rall. Electrophysiology of a dendritic neuron model. *Biophysic. J.*, 2(2):145–167, 1962.

[46] L.M. Ricciardi. Diffusion approximation for a multi-input model neuron. *Biol. Cybernetics*, 24:237–240, 1976.

[47] L.M. Ricciardi. On the transformation of diffusion processes into the Wiener process. *J Math Analysis and Appl*, 54(1):185–199, 1976.

[48] L.M. Ricciardi, A. Di Crescenzo, V. Giorno, and A.G. Nobile. An outline of theoretical and algorithmic approaches to first passage time problems with applications to biological modeling. *Math. Japon.*, 50(2):247–322, 1999.

[49] L.M. Ricciardi and L. Sacerdote. The Ornstein-Uhlenbeck process as a model for neuronal activity. *Biol. Cybernetics*, 35:1–9, 1979.

[50] L.M. Ricciardi and S. Sato. Diffusion processes and first-passage-time problems. In *Lectures in applied mathematics and informatics*, pages 206–285. Manchester Univ. Press, Manchester, 1990.

[51] J. Rinzel and W. Rall. Transient response in a dendritic neuron model for current injected at one branch. *Biophys. J.*, 14:759–790, 1974.

[52] L. Sacerdote and R. Sirovich. *A Wiener process with Inverse Gaussian time distributed jumps as a model for neuronal activity.* V.Capasso Editor, 2002.

[53] L. Sacerdote and R. Sirovich. Multimodality if the interspike interval distribution in a simple jump-diffusion model. *Scientiae Mathematicae Japonicae*, 8:359–374, 2003.

[54] G. Sampath and S.K. Srinivasan. *Stochastic Models for Spike Trains of Single Neurons*, volume 16 of *Lecture Notes in Biomathematics.* Springer-Verlag, 1977.

[55] J. K. Seamans, N. A. Gorelova, and C. R. Yang. Contributions of voltage-gated Ca2+ channels in the proximal versus distal dendrites to synaptic integration in prefrontal cortical neurons. *The Journal of Neuroscience*, 17(15):5936–5948, August 1997.

[56] G. M. Shepherd. *Neurobiology*. Oxford University Press, USA, 3 edition edition, May 5 1994.

[57] T. Shimokawa, K. Pakdaman, and S. Sato. Time-scale matching in the response of a leaky integrate-and-fire neuron model to periodic stimulus with additive noise. *Phys. Rev. E*, 59:3427–3443, 1999.

[58] A.N. Shiryaev. *Probability*, volume 95 of *Graduate Texts in Mathematics*. Springer-Verlag, New York, second edition, 1996. Translated from the first (1980) Russian edition by R. P. Boas.

[59] R. Sirovich and L. Sacerdote. Noise induced phenomena in jump diffusion models for single neuron spike activity. *Proceedings IJCNN 2004*, 2004.

[60] R Sirovich, L. Sacerdote, and A.E.P. Villa. Multimodal inter-spike interval distribution in a jump-diffusion neuronal model. Submitted to Journal of Computational Neuroscience, 2005.

[61] R. Sirovich and C. Zucca. Multidimensional bridges with application to the integrated brownian motion. PrePrint, 2005.

[62] R.B. Stein. A theoretical analysis of neuronal variability. *Biophys. J.*, 5:173–193, 1965.

[63] I.V. Tetko and A.E.P. Villa. A pattern gouping algorithm for analysis of spatiotemporal patterns in neuronal spike trains. 1.detection of repeated patterns. *J. Neurosci. Methods*, 105:1–14, 2001.

[64] I.V. Tetko and A.E.P. Villa. A pattern gouping algorithm for analysis of spatiotemporal patterns in neuronal spike trains. 2.application to simultaneous single unit recordings. *J. Neurosci. Methods*, 105:15–24, 2001.

[65] R. F. Thompson. *The brain: a neuroscience primer*. Worth Publishers, 3rd edition edition, March 29 2000.

[66] H.C. Tuckwell. *Introduction to theoretical neurobiology. Vol. 1*, volume 8 of *Cambridge Studies in Mathematical Biology*. Cambridge University Press, Cambridge, 1988. Linear cable theory and dendritic structure.

[67] H.C. Tuckwell. *Introduction to theoretical neurobiology. Vol. 2*, volume 8 of *Cambridge Studies in Mathematical Biology*. Cambridge University Press, Cambridge, 1988. Nonlinear and stochastic theories.

[68] S.R. Williams and G.J. Stuart. Dependence of epsp efficacy on synapse location in neocortical pyramidal neurons. *Science*, 295:1907–10, 2002.

[69] S.R. Williams and G.J. Stuart. Role of dendritic synapse location in the control of action potential output. *Trends in Neurosci.*, 26(3):147–154, 2003.